Molecular Vision 2024; 30:239-259 <http://www.molvis.org/molvis/v30/239>
Received 18 July 2023 | Accepted 28 June 2024 | Published 1 July 2024

Retinal and metabolic changes in a high-fat diet (HFD)+STZ model of Type II diabetes

Stephen Phillips,[1,2] Andrew Feola,[1,2,3] Jessica Solomon,[1,4] Lidia Cardelle,[1,2] Amber Douglass,[1] Katie L. Bales,[1,3] Monica Coulter,[1] Lauren Hutson,[1] Cara T. Khayat,[1,2] Ally Grubman,[1,4] Cody Worthy,[1] Jeffrey H. Boatright,[1,3] Machelle T. Pardue,[1,2,3] Rachael S. Allen[1,2]

[1]Center for Visual and Neurocognitive Rehabilitation, Joseph M Cleland Atlanta VA Medical Center, Decatur, GA; [2]Department of Biomedical Engineering, Georgia Institute of Technology, Atlanta, GA; [3]Department of Ophthalmology, Emory University, Atlanta, GA; [4]Department of Neuroscience & Behavioral Biology, Emory University, Atlanta, GA

While the high-dose streptozotocin (STZ; 100 mg/kg) rodent model is the gold standard in modeling Type I diabetes, models for Type II diabetes are needed for this more common form of diabetes. We investigated the retinal, cognitive, and metabolic alterations in a Type II diabetic model induced by high-fat diet (HFD) and low-dose STZ (30 mg/kg). Long Evans rats were assigned to naïve control, HFD, or HFD+STZ groups. Diabetic rats were further stratified into Type I and Type II based on metabolic assessments. Optomotor response (OMR, visual function), electroretinograms (retinal function), and Y-maze (cognitive function) were tested. Serum was analyzed for 12 metabolic markers using a multiplex panel. Type I rats showed severe increases in blood glucose accompanied by impairments in insulin and glucose tolerance, reduced bodyweight, and low insulin levels. In contrast, Type II rats showed moderate changes in blood glucose and insulin and glucose tolerance with weights and insulin levels similar to naïve controls. Type I and II rats showed OMR deficits ($p<0.05$) and electroretinogram changes ($p<0.05$). No cognitive deficits were observed. Type I rats displayed reduced serum levels of brain-derived neurotrophic factor (BDNF), C-Peptide, and leptin ($p<0.05$), and alterations in C-Peptide, PYY, and glucagon levels correlated with retinal function changes ($p<0.05$). Type II rats exhibited a moderate diabetic state while still developing retinal and visual deficits, which recapitulates phenotypes reported in patients.

The estimated prevalence of diabetes in the United States has increased from 10.3% in 2001–2004 to 13.2% in 2017–2020 (Prevalence of Both Diagnosed and Undiagnosed Diabetes, CDC). Globally, 537 million adults live with diabetes, a number that is predicted to rise over the next 10 years (IDF Atlas, 10th Edition). Less than 10% of these individuals have Type I diabetes, which is characterized by the autoimmune loss of β-cells in the pancreas and a consequent rise in blood glucose levels due to decreased insulin production [1,2]. The remaining 90%–95% of these individuals suffer from Type II diabetes, which occurs when β-cells can no longer produce enough insulin to compensate for the development of insulin resistance [1,3]. Additionally, the chronic hyperglycemia and inflammation that accompany diabetes can result in the development of diabetic retinopathy (DR), which is a leading cause of blindness in adults in the United States (Common Eye Disorders and Diseases) [4-6], affecting over 93 million people worldwide [7]. The high prevalence and projected increase in cases of diabetes require a better understanding of the mechanisms and impacts of this disease to reduce diabetes-related complications.

Animal models have been invaluable tools for further understanding the pathology and complexity of diabetes. The most common and well established experimental model of diabetic retinopathy and neuropathy in Type I diabetes uses a systemic injection of high-dose streptozotocin (STZ, 100 mg/kg) in rats to ablate pancreatic β-cells [8,9]. Streptozotocin is a toxic analog of glucose that induces the apoptosis of β-cells in the pancreas through DNA methylation and oxidative stress [10,11], resulting in a hyperglycemia model that remarkably mimics the complications of Type I diabetes [1]. For Type II diabetes, multiple models have been developed, including the Goto–Kakizaki (GK) rat [12,13], the Akita mouse [14,15], rodents with leptin mutations [16,17], and diet-induced obesity models [18,19]. Unfortunately, unlike the model for Type I, no such gold standard model exists for Type II diabetes. Therefore, a model that replicates the clinical symptoms and complications of Type II diabetes, including diabetic retinopathy, is needed.

The high-fat diet (HFD) + low-dose STZ (30 mg/kg) rodent model recapitulates many of the features of both Type II diabetes and consequent DR, including the development

Correspondence to: Rachael S. Allen, Atlanta VA Center for Visual and Neurocognitive Rehabilitation,Research Service (151 Oph),1670 Clairmont Rd, Decatur, GA 30033; Phone: (404) 321-6111 X207570; FAX: (404) 728-4847; email: restewa@emory.edu

of hyperglycemia and inflammation, increased triglyceride and cholesterol levels, and decreased retinal function [20-26]. Rather than a single high dose of STZ, this model combines a HFD (40% kcal from fat) with 1 to 3 low doses of STZ. Long Evans rats—an outbred strain developed by breeding Wistar female and wild gray male rats—were used in this study. As an outbred strain, these rats are easily available, relatively inexpensive, and more genetically diverse compared with inbred or genetically modified strains like the previously used spontaneously-hypersensitive rat (SHR) [20]. Finally, in addition to simulating the natural disease progression and pathophysiology of Type II diabetes, the HFD-STZ model has proven suitable for testing antidiabetic compounds [21]. Previous research has identified a time course for retinal deficits in a Type II diabetic rodent model [27]. However, to our knowledge, only one study to date has used behavioral assessments to evaluate visual function following the administration of a high-fat, high-sucrose (HFHS) diet, and results indicated no significant changes in spatial frequency thresholds [28]. Additionally, no prior research has evaluated the time course of cognitive deficits in the HFD-STZ model following retinal complications.

The purpose of the present study was to further characterize an HFD plus low-dose STZ Type II model of diabetes for early retinal dysfunction and delineate the time course of retinal and cognitive disruption associated with the HFD-STZ rodent model. Additionally, we assessed serum metabolic markers and determined whether these correlated with retinal changes. We hypothesized that Type II rats would develop significant cognitive, retinal, and visual deficits while maintaining a moderate diabetic state with sustained insulin secretion.

METHODS

Animals and experimental design: Adult male Long Evans rats (Charles River, Wilmington, MA; 42 days old; n=44) were housed in shoe-box style cages and had continuous access to food and water. The cohort was kept on a 12:12, light:dark cycle, with light onset at 6:00 AM The Atlanta Veterans Affairs Institutional Animal Care and Use Committee approved all procedures, and protocols conformed to the Association for Research in Vision and Ophthalmology (ARVO) Statement for the Use of Animals in Ophthalmic and Vision Research and the National Institutes of Health Guide for the Care and Use of Laboratory Animals (NIH Publications, 8th edition, updated 2011). Rats were randomly assigned to three groups: naïve control (n=12), HFD (n=14), and HFD + low-dose STZ (n=17). Glucose tolerance and insulin tolerance tests were performed at 2 weeks post-hyperglycemia to evaluate the glycemic response and insulin sensitivity, respectively. Optomotor response (OMR) was used to assess visual function every 2 weeks from baseline, and electroretinogram (ERG) recordings were performed at 4 and 8 weeks post-hyperglycemia to assess retinal function. Y-maze was used to assess cognitive function every 4 weeks from the baseline. Rats were euthanized at 10 weeks post-hyperglycemia, and retinas and serum were taken for multiplex analysis of metabolic biomarkers. Figure 1 outlines the schedule of diet and assessments.

HFD + STZ model: Rats were assigned to one of the following groups: naïve control, HFD, or HFD+STZ, 1 week after animal delivery. The HFD groups were fed an adjusted fat diet with a 40% kcal formula from fat (Envigo, Madison, WI). Naïve control rats were fed a standard rat diet with 18% kcal from fat. Normally, 100 mg/kg of STZ is used to create a Type I diabetic rat model [29]. In this study, after 4 weeks of HFD, the HFD+STZ group received a single dose of STZ (30 mg/kg) once a week for 1–3 weeks. Rats with a blood glucose level of <140 mg/dl after the first injection were given a second injection. Rats with a blood glucose level of <140 mg/dL after the second injection were given a third injection. Of the rats that became diabetic, this smaller amount of STZ in combination with the HFD yielded 9 of 18 Type II diabetic rats and 8 of 18 Type I diabetic rats (Type I versus II classification methodology has been provided below). One rat did not become hyperglycemic and was excluded from the study.

Our methods for classifying the rats as Type I, Type II, or nondiabetic are described here and in the flowchart in Figure 2. Rats with an average blood glucose level greater than 250 mg/dL were considered to model Type I diabetes and remained in this study for comparison. Rats with a blood glucose level of less than 250 mg/dL but greater than 140 mg/dL were considered to model Type II diabetes. Weights, glucose and insulin tolerance, and serum insulin levels were used to confirm the rats' status as Type I or Type II. Weights and insulin levels were useful in confirming whether rats in the 200–250 mg/dL range were Type I or Type II. Rats in this range that had a large drop in weight and severely low insulin levels were considered Type I. A glucose tolerance test was useful in confirming whether rats in the 105–150 mg/dL range were Type II or nondiabetic. Rats in this range with a similar glucose tolerance response to the confirmed Type II rats were considered Type II as well.

Weights and average blood glucose level: Throughout the study, the rats were weighed on a benchtop scale (PM2000, Mettler-Toledo, Columbus, OH) and blood glucose levels were checked weekly. The blood glucose measurements were taken by a handheld blood glucose meter (FreeStyle Lite, Abbott

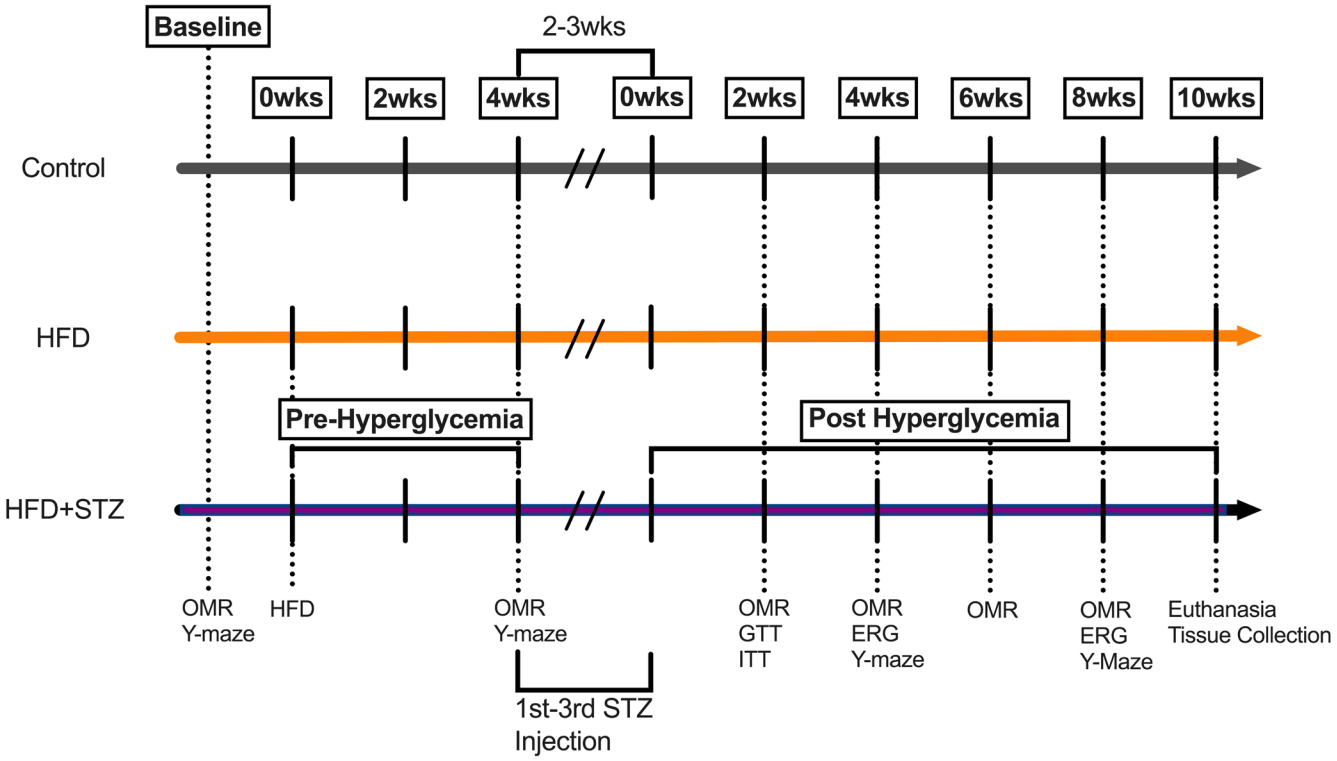

Figure 1. Timeline of treatments and assessments. After baseline measurements, a high-fat diet (HFD) was given to the rats that would comprise the HFD and the HFD+streptozotocin (STZ) groups. After 4 weeks on HFD, the HFD+STZ group received 2–3 injections of STZ over the course of 2–3 weeks. The rats were then followed for 8 weeks with assessments performed as depicted above. The rats were euthanized at 10 weeks post-hyperglycemia. The assessments were optomotor response (OMR), Y-maze performance, glucose tolerance test (GTT), insulin tolerance test (ITT), and electroretinograms (ERG).

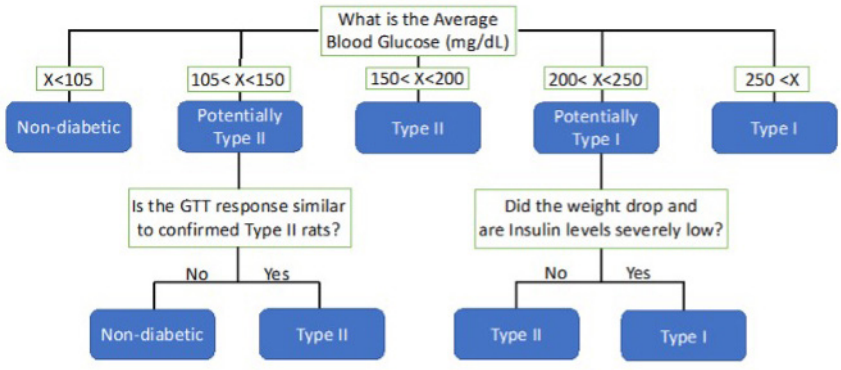

Figure 2. Flowchart for how diabetic rats were classified as Type I or Type II or non-diabetic. Biweekly blood glucose measurements were averaged post-euthanasia. If the average blood glucose level was less than 105 mg/dl, the rat was classified as nondiabetic. If the average blood glucose level was between 105 and 150 mg/dl, the glucose tolerance test results were used to determine if the rat's response was closer to the control group or the Type II group. If the average blood glucose level was between 150 to 200 mg/dl, the rat was classified as Type II. If the average blood glucose level was between 200 to 250 mg/dl, the insulin levels and weight data were used. If the insulin levels were less than 1 ng/ml and the rat had a significantly lower bodyweight, they were classified as Type I. However, if insulin levels and bodyweight did not significantly change the rat was classified as Type II.

Diabetes Care, Alameda, CA) and test strips. Preceding this, the tail was wiped to remove urine and then pricked with a small syringe. The average was calculated from 1 week after the last STZ injection through the week of euthanasia.

ELISA for serum insulin levels: Rats were euthanized at 10 weeks post-hyperglycemia and blood samples were obtained. Blood samples were centrifuged at 10,000 g for 10 min, and the serum was transferred to a new tube and stored at −80 °C until use. A bicinchoninic acid (BCA) protein assay kit (Pierce BCA Protein Assay Kit, Catalog No. PI23225) was used to measure total protein concentration, and a plate reader (BioTek Synergy 2, Agilent Technologies, Santa Clara, CA) was used to measure the absorbance at 562 nm.

Serum insulin levels were evaluated using an ELISA kit tailored to insulin (Rat Ultrasensitive Insulin, Alpco, Catalog No. 80-INSRTU-E01). Standards and samples (5 µl) were run in triplicates according to the manufacturer's instructions. A plate reader (BioTek Synergy 2, Agilent Technologies, Santa Clara, CA) was used to measure the absorbance at 450 nm. The standard concentration and absorbance measurements were used to determine the sample concentration with a four-parameter nonlinear regression using image analysis software (BioTek Gen5, Agilent Technologies, Santa Clara, CA). Results were expressed as the concentration of insulin (ng/mL).

Glucose and Insulin tolerance tests: At 2 weeks post-hyperglycemia, glucose tolerance tests (GTT) and insulin tolerance tests (ITT) were used to gauge hyperglycemia and insulin resistance, respectively. Before the assessment, the rats were fasted for 6 h. An intraperitoneal injection of glucose (2 mg/kg bodyweight) in dH_2O was given to the rats for GTT. Blood glucose levels (mg/dL) were monitored at 0, 15-, 30-, 60-, and 120 min using test strips via a tail prick and handheld blood glucose meter (FreeStyle Lite, Abbott Diabetes Care, Alameda, CA). For ITT, an insulin injection (0.35 units/kg bodyweight) was given to the rats intraperitoneally. Thereafter, blood glucose levels were monitored at 0, 15-, 30-, and 60- min.

Optomotor response (OMR): To assess visual function, an optomotor response system (OptoMotry; Cerebral-Mechanics, Lethbridge, AB, Canada) was used, as previously described [29]. Rats were placed on a pedestal in the middle of a virtual reality chamber made of four flatscreen monitors that display vertical sine wave gratings rotating at a speed of 12 deg/s The rats were monitored in real time by the experimenter with a video camera. Rats exhibited either the presence or absence of a reflexive head movement (tracking) in response to the rotating gratings moving in a clockwise or counter-clockwise direction. The OptoMotry software automatically calculates the spatial frequency (SF) and contrast sensitivity (CS) thresholds using a staircase paradigm. When assessing SF, initial gratings had an SF of 0.042 cyc/deg with 100% contrast, and the SF changed over time based on the rat's tracking response (or lack thereof) while the contrast remained constant. When assessing CS, initial gratings had 100% contrast, which decreased or increased based on the rat's tracking. SF was held constant during CS assessments at 0.064 cy/deg, which is peak SF for rats at baseline [30]. Contrast sensitivity values reported here were calculated as a reciprocal of the Michelson contrast using the screens' luminance (i.e., [maximum + minimum] / [maximum – minimum]), as described previously [31].

Electroretinogram: Electroretinogram was used to measure the response of retina to light, as previously described [32,33]. Rats were dark adapted overnight. Under red light, rats were anesthetized with ketamine (60 mg/kg) and xylazine (7.5 mg/kg). The corneal surface was anesthetized with 0.5% tetracaine and pupils dilated with 1% tropicamide. Reference electrodes made of platinum were placed in the tail and in each cheek. Custom-made gold loop recording electrodes were placed on each cornea. A signal-averaging system (UTAS BigShot; LKC Technologies, Gaithersburg, MD) was used to record the retinal response to different flash stimuli. A six-step protocol of flash stimuli presented in order of increasing luminance was used, and five dark-adapted responses were recorded (scotopic: −3.0 to 2.1 log cd s/m^2). Following the dark-adapted steps, rats were light-adapted for 10 min at 30 cd/m^2 to saturate rod photoreceptors. Afterwards, flicker stimuli (2.0 log cd s/m^2 at 6 Hz) were presented in the presence of background light to measure cone pathway function. Finally, to reverse the effects of xylazine, rats were given atipamezole after the ERGs [34].

The responses from the left and right eye were averaged. Amplitudes and implicit times were measured for a- waves, b- waves, and oscillatory potentials (OPs), and flicker ERG waveforms. The OPs were filtered digitally (75–500 Hz; EM Version 8.1.2, 2008; LKC Technologies) using the ERG system software and analyzed (flash stimuli: −1.9 log cd s/m^2).

Y-Maze: Cognitive ability and exploratory behavior were assessed using a Y-maze (San Diego Instruments, San Diego, CA) [35]. To conduct this test, rats were placed one at a time in the same arm of the maze. Each rat had a period of 8 min to explore the maze. Exploratory behavior was measured by the total number of times a rat entered an arm during its trial. Cognitive ability was assessed through spontaneous alternation—a measure of spatial memory. An alternation occurs when a rat enters the three arms consecutively. Spontaneous

alternation was calculated by the number of alternations (A) divided by (the total arm entries (E) minus 2), that is, A/(E−2).

Multiplex assay: A multiplex assay was used to assess metabolic biomarkers, including brain-derived neurotrophic factor (BDNF), connecting peptide (C-Peptide), fibroblast growth factor 21 (FGF-21), ghrelin (active and total), glucagon-like peptide 1 (GLP-1; active, inactive, and total), glucagon, insulin, leptin, and peptide tyrosine-tyrosine (PYY; total). Serum samples were assayed through a multiplex kit as per the manufacturer's instructions (U-PLEX Rat Metabolic Combo 1, Meso Scale Delivery, Rockville, MD). The detection antibody solution was made by combining 60 µL of each detection antibody, 180 µL of MSD Blocker D-R, and 5.1 ml of eluent 11 to bring the total volume to 6 ml. Once the detection antibody solution was made, 50 µl of calibrator standard was added to each well of a 96-well plate and sealed. The plate was then incubated for 2 h at room temperature (approximately 21 °C) while being shaken. Once incubated, each well was washed 3 times with 150 µl of 1XPBS-T, and 50 µl of the detection antibody solution was added. The plate was sealed again and incubated for 1 h at room temperature (approximately 21 °C) while shaking. The 3 final wash steps were performed with 150 µl of 1XPBS-T per well. Lastly, 150 µl of MSD GOLD Read Buffer B was added to each well and the plate was analyzed on a MESO Quickplex SQ 120 (Meso Scale Delivery, Rockville, MD).

Statistical analysis: Results are represented as mean ± standard error of the mean (SEM). Weight, GTT, ITT, OMR (spatial frequency and contrast sensitivity), ERG (a-wave and b-wave), and Y-maze (spontaneous alternation and the number of entries) results were analyzed using a two-way repeated-methods (RM) ANOVA followed by the Holms−Sidak tests for individual comparisons. Average blood glucose results over time, ELISA for serum insulin levels, OPs, and multiplex results were analyzed using a one-way ANOVA followed by the Holms−Sidak tests for individual comparisons. Correlations of visual and retinal changes to the metabolic biomarkers were analyzed using Pearson's correlation. Outlier tests were performed using the ROUT method on the multiplex data. Two outliers were removed in the multiplex data for leptin and one was removed for glucagon. For multiplex results and correlations, comparisons were performed with the α level corrected for false discovery rate ($p<0.026$) [36], which is why a more stringent α criterion than the commonly used 0.05 is employed here.

RESULTS

Type II rats exhibited a different metabolic phenotype than Type I, HFD, or naïve control rats: As expected, average blood glucose levels for Type I rats (391.70±20.59 mg/dL) were significantly higher than those for every other group ($p<0.0001$; Figure 3A). In contrast, blood glucose values for Type II rats (163.37±15.42 mg/dL) were more moderate, showing averages that were significantly higher than HFD (88.16±1.61 mg/dL) and naïve control rats (82.62±1.93 mg/dL) as well as significantly lower than Type I rats ($p<0.0001$ for all three comparisons; ANOVA, $F_{3,39}=178.3$; $p<0.0001$; Figure 3A). Type II rats showed similar serum insulin levels (3.76±0.50 ng/mL) to control (4.68±0.24 ng/mL) and HFD rats (4.72±0.36 ng/mL). Meanwhile, Type I rats had significantly lower serum insulin levels (0.43±0.098 ng/mL) compared to every other group ($p<0.0001$; ANOVA, $F_{3,37}=26.84$; $p<0.0001$; Figure 3B).

For Type II rats (619.5±36.65 g), there was no significant weight difference in comparison to the control rats (580.75±15.44 g, 6.67%), or in comparison to the HFD rats (655.0±26.31 g, −5.42%; Figure 3C). The Type I rats, however, weighed significantly less (417.6±8.96 g, −28.09%) than the other three groups ($p<0.05$ at 9 weeks, $p<0.001$ at 10 weeks, and $p<0.0001$ at 11 through 16 weeks compared with Type II rats) from week 9 through the rest of the experiment (RM ANOVA interaction effect, group*time point, $F_{42,555}=3.821$; $p<0.0001$; Figure 3C). Additionally, the HFD rats weighed significantly more (12.79%) than the controls ($p<0.05$ to $p<0.01$ for weeks 8 and 10–16).

Type II rats exhibited moderate glucose and insulin intolerance: During the GTT, Type II rats exhibited a significantly higher blood glucose level (203.3%) at the 30-, 60-, and 120-min time points when compared to control rats ($p<0.01$ at 30 min, $p<0.0001$ at 60 min, and $p<0.01$ at 120 min; RM ANOVA main effect of group, $F_{3,130}=29.87$; $p<0.0001$; Figure 4A). Type II rats had a significantly increased blood glucose level at the 30- and 60-min time points in comparison to the HFD rats ($p<0.05$ at 30 min and $p<0.01$ at 60 min; Figure 4A). Type II rats also showed a significantly lower blood glucose level at all time points when compared to the Type I rats ($p<0.001$ at 0 min, $p<0.0001$ at 15-, 30-, and 120 min, and $p<0.01$ at 60 min; Figure 4A). Type I rats showed a significant increase in blood glucose level (299.4%) at all time points when compared to control rats ($p<0.0001$ at 0, 15-, 30-, 60-, and 120 min; Figure 4A). The HFD rats had a significant increase in blood glucose level only at the 60-min time point in comparison to the control rats ($p<0.05$; Figure 4A).

During the insulin tolerance test, Type II rats had a significantly higher blood glucose level at the 0- and 15-min

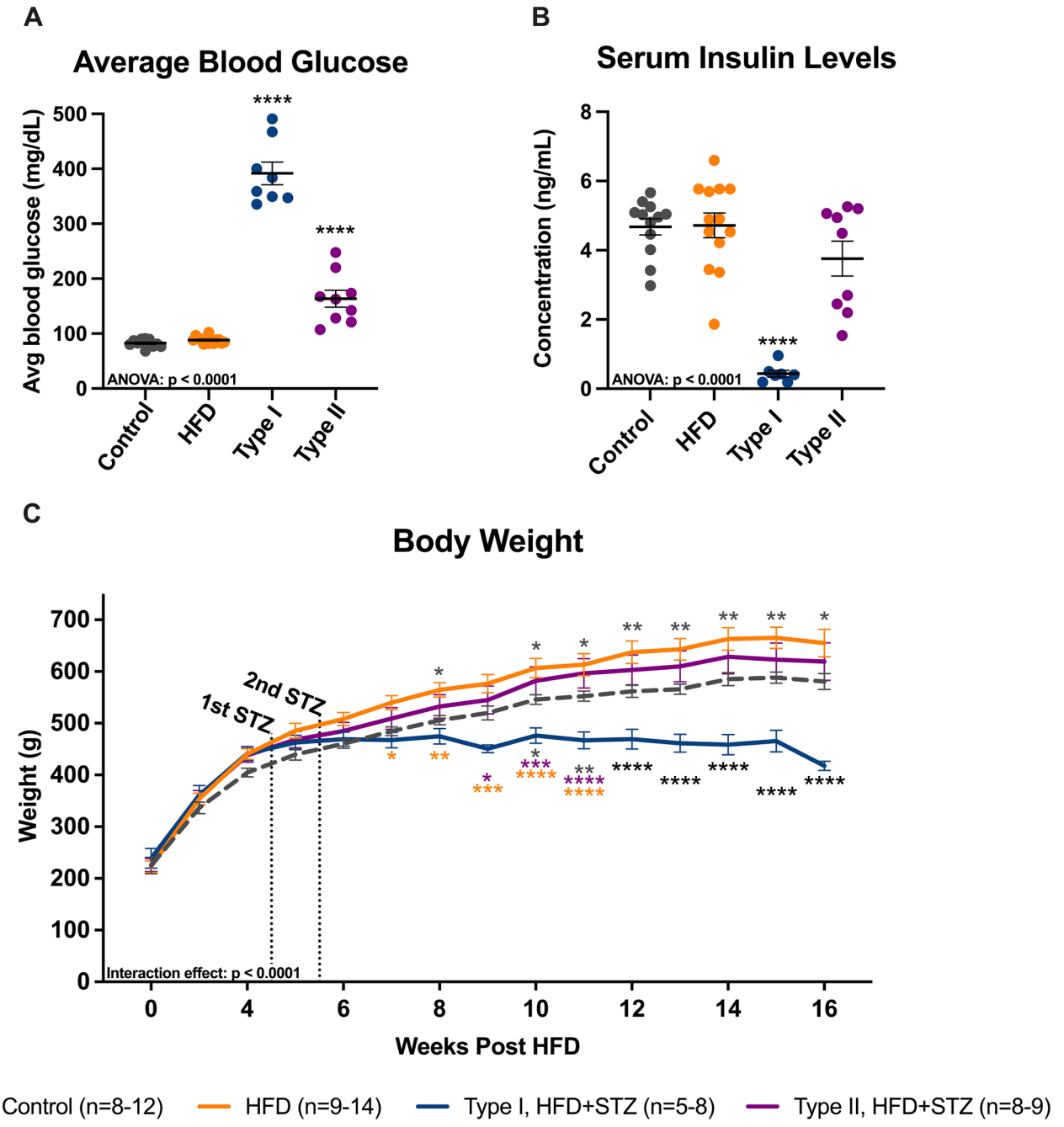

Figure 3. Type II rats maintained a normal bodyweight, were moderately hyperglycemic, and had no significant drop in serum insulin levels. **A**: Average blood glucose levels from weekly measurements. **B**: Serum insulin levels detected by an ELISA from serum collected post-euthanasia. **C**: Weights of rats taken weekly. The colored asterisks correspond to a significant difference with the group that shares the color of the asterisks. Black asterisks mean a significant difference with every other group. * p<0.05, ** p<0.01, *** p<0.001, **** p<0.0001. Results expressed as mean ± SEM.

time points when compared to the control rats (p<0.0001 at 0 min and p<0.05 at 15 min; RM ANOVA interaction effect, group*time post-insulin, F9,108=17.08; p<0.0001; Figure 4B). Type II rats also had a significantly higher blood glucose level compared to the HFD rats at the 0-min time point but did not have a significant difference for the other time points (p<0.05 at 0 min; Figure 4B). Type I rats had a significantly higher blood glucose level compared to all other groups at the 0-, 15-, and 30-min time points (p<0.0001 at 0 and 15 min, p<0.01 to p<0.001 at 30 min; Figure 4B). However, at the 60-min time point, the blood glucose level of Type I rats was only significantly higher than that of the control group rats (p<0.05; Figure 4B).

Reduced visual function was observed in diabetic and HFD rats: Type II rats showed significant reductions in spatial frequency beginning at 4 weeks post-HFD/0 weeks post-STZ (p<0.05) compared with control rats (RM ANOVA interaction effect, group*time point, F15,230=10.56; p<0.0001; Figure 5A). Similar deficits were observed in Type I rats beginning at 6 weeks post-HFD/2 weeks post-STZ (p<0.05). Smaller, but still significant, deficits were observed in HFD rats beginning at 6 weeks post-HFD (p<0.05). For contrast sensitivity, significant reductions were observed in Type II, Type I, and HFD rats compared with controls (RM ANOVA interaction effect, group*time point, F15,230=2.446; p<0.01; Figure 5B) with different times of onset for each group. Specifically, Type II rats showed reductions beginning at 8 weeks post-HFD/4 weeks post-STZ (p<0.05), Type I rats showed reductions beginning at 6 weeks post-HFD/2 weeks post-STZ (p<0.05), and HFD rats showed reductions beginning at 8 weeks post-HFD (p<0.05).

Type II rats showed delayed electroretinogram (ERG) implicit times, while Type I rats showed reduced ERG amplitudes: For Type II rats, a significant delay in oscillatory potential implicit times (IT) at 8 weeks post-STZ was observed in response to dim stimuli when compared to control rats for OP2 (ANOVA, F3,38=4.123; p<0.05; Figure 6B), OP3 (ANOVA, F3,38=5.886; p<0.01; Figure 6C), and OP4 (ANOVA, F3,38=4.146; p<0.05; Figure 6D). Meanwhile, Type I rats had reduced a-wave (RM ANOVA main effect of group, F3,136=5.811; p<0.001; Figure 7A), b-wave (RM ANOVA main effect of group, F3,190=17.44; p<0.0001; Figure 7B), and flicker amplitudes (ANOVA, F3,38=4.019; p<0.05; Figure 7C) at 8 weeks post-STZ (Figure 7). No significant findings

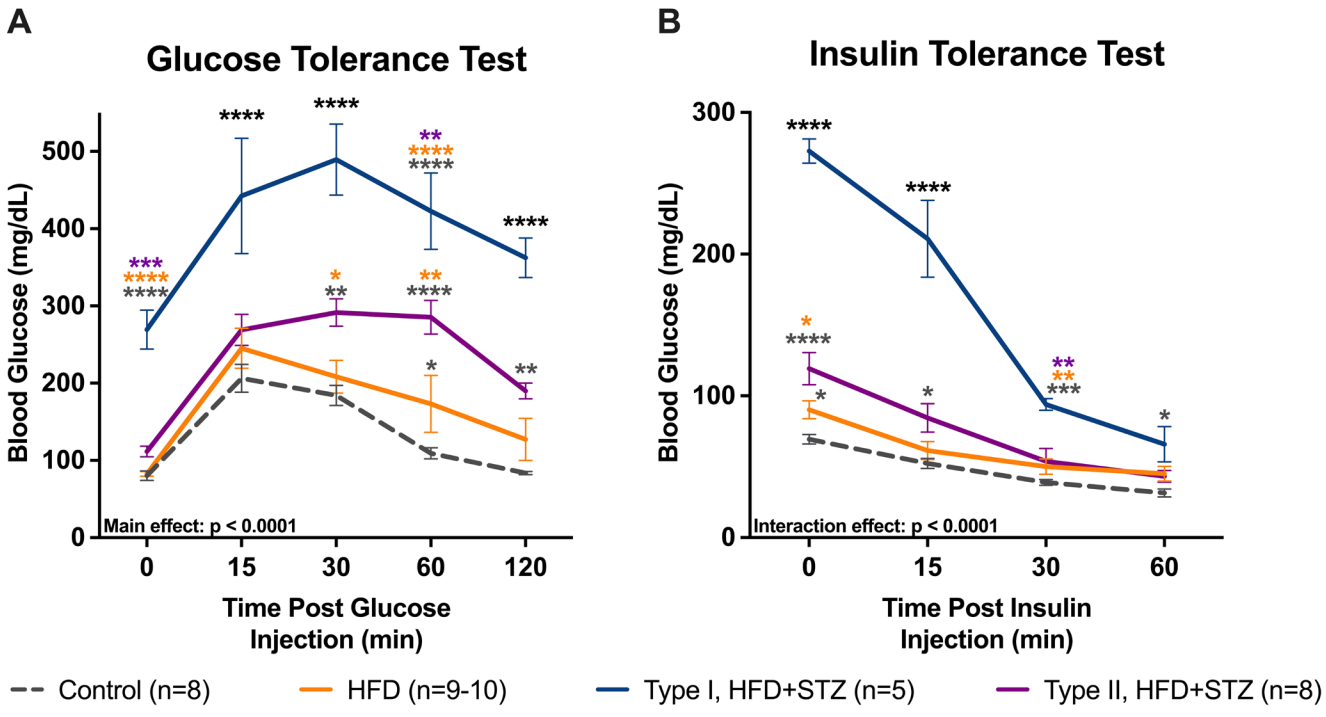

Figure 4. Type II diabetic rats express moderately worse glucose and insulin tolerance. **A**: Glucose response curves from glucose tolerance tests performed at 2 weeks post-hyperglycemia. **B**: Glucose response curves from insulin tolerance tests performed at 2 weeks post-hyperglycemia. The colored asterisks correspond to a significant difference with the group that shares the color of the asterisks. Black asterisks correspond to a significant difference with every other group. * p<0.05, ** p<0.01, *** p<0.001, **** p<0.0001. Results expressed as mean ± SEM.

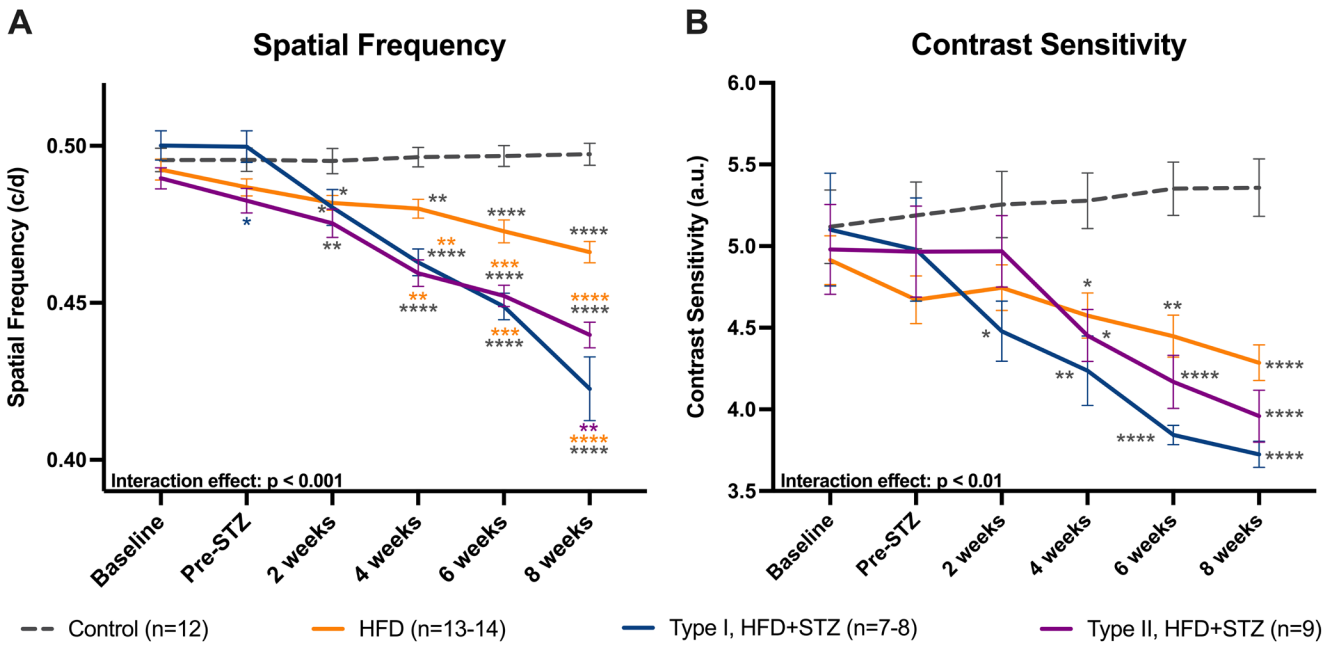

Figure 5. Type II rats showed deficits in both spatial frequency and contrast sensitivity. **A**: Spatial frequency and (**B**) contrast sensitivity assessed through optomotor response at baseline, pre-STZ, 2-, 4-, 6- and 8-weeks post-hyperglycemia. The colored asterisks correspond to a significant difference with the group that shares the color of the asterisks. Black asterisks correspond to a significant difference with every other group. * p<0.05, ** p<0.01, *** p<0.001, **** p<0.0001. Results expressed as mean ± SEM.

were observed for OP1 implicit time (Figure 6A) in response to dim stimuli, for OP1–4 amplitudes in response to dim or bright flash stimuli, for OP1–4 implicit times in response to bright flash stimuli, or for a-wave and b-wave implicit time (data not shown).

No changes in cognitive behavior were observed through 8 weeks: Type I, Type II, and HFD rats did not show deficits in cognitive (spontaneous alternation) or exploratory behavior, as measured by Y-maze, during the time points assessed here (Figure 8).

Diabetic rats displayed alterations in metabolic biomarkers that correlated with retinal and visual changes: Serum alterations in multiple metabolic biomarkers were observed in blood collected post-euthanasia, particularly in Type I rats (Figure 9A). Specifically, Type I rats showed significant reductions in serum levels of BDNF (ANOVA, $F_{3,36}=2.913$; $p<0.026$; Figure 9B), C-Peptide (ANOVA, $F_{3,36}=7.704$; $p<0.001$; Figure 9C), and leptin (ANOVA, $F_{3,34}=2.937$; $p<0.01$; Figure 9D). The HFD rats showed a significant decrease in serum levels of PYY (ANOVA, $F_{3,36}=4.607$; $p<0.01$, Figure 9E). Additionally, a main effect of group was observed for FGF-21 (ANOVA, $F_{3,36}=4.028$; $p<0.026$, Figure 9F), with higher levels appearing in HFD and Type II rats. Trends for reductions in glucagon were observed in Type I and Type II rats ($p=0.0657$, Figure 9G).

Serum changes showed mild correlations with visual changes. Specifically, changes in spatial frequency at 8 weeks correlated with serum levels of C-Peptide ($R2=0.1655$; $p<0.01$; Figure 10B), PYY ($R2=0.1534$; $p<0.026$; Figure 10C), and glucagon ($R2=0.1899$; $p<0.01$; Figure 10D), with a trend for changes in leptin ($R2=0.1221$; $p=0.0315$; Figure 10A). Changes in contrast sensitivity at 8 weeks correlated with serum levels of PYY ($R2=0.2624$; $p<0.001$; Figure 10E) and glucagon ($R2=0.1552$; $p<0.026$; Figure 10F). For details on statistical analysis, including why an α level of 0.026 rather than 0.05 was used, please see the Methods section.

DISCUSSION

Type I and Type II HFD+STZ rats exhibited distinct diabetic metabolic phenotypes: Our use of the HFD + low-dose STZ model resulted in two distinct diabetic metabolic phenotypes, with Type II rats exhibiting a moderate diabetic state as demonstrated by moderate increases in blood glucose and moderate impairment in glucose tolerance, in addition to weights and serum insulin levels similar to naïve controls. In contrast, rats classified as Type I in this study showed large increases in blood glucose and impairment in glucose

tolerance coupled with decreases in bodyweight and very low insulin levels.

Type II rats had no significant differences in their weights compared to the control rats, which is revealing about their overall condition, as more severe diabetic animals tended to lose weight throughout the course of the study [21]. The moderate hyperglycemia observed in Type II rats in conjunction with little to no drop in serum insulin was also observed in previous studies [20,21]. Type II rats also had both impaired glucose and insulin tolerance, a finding which

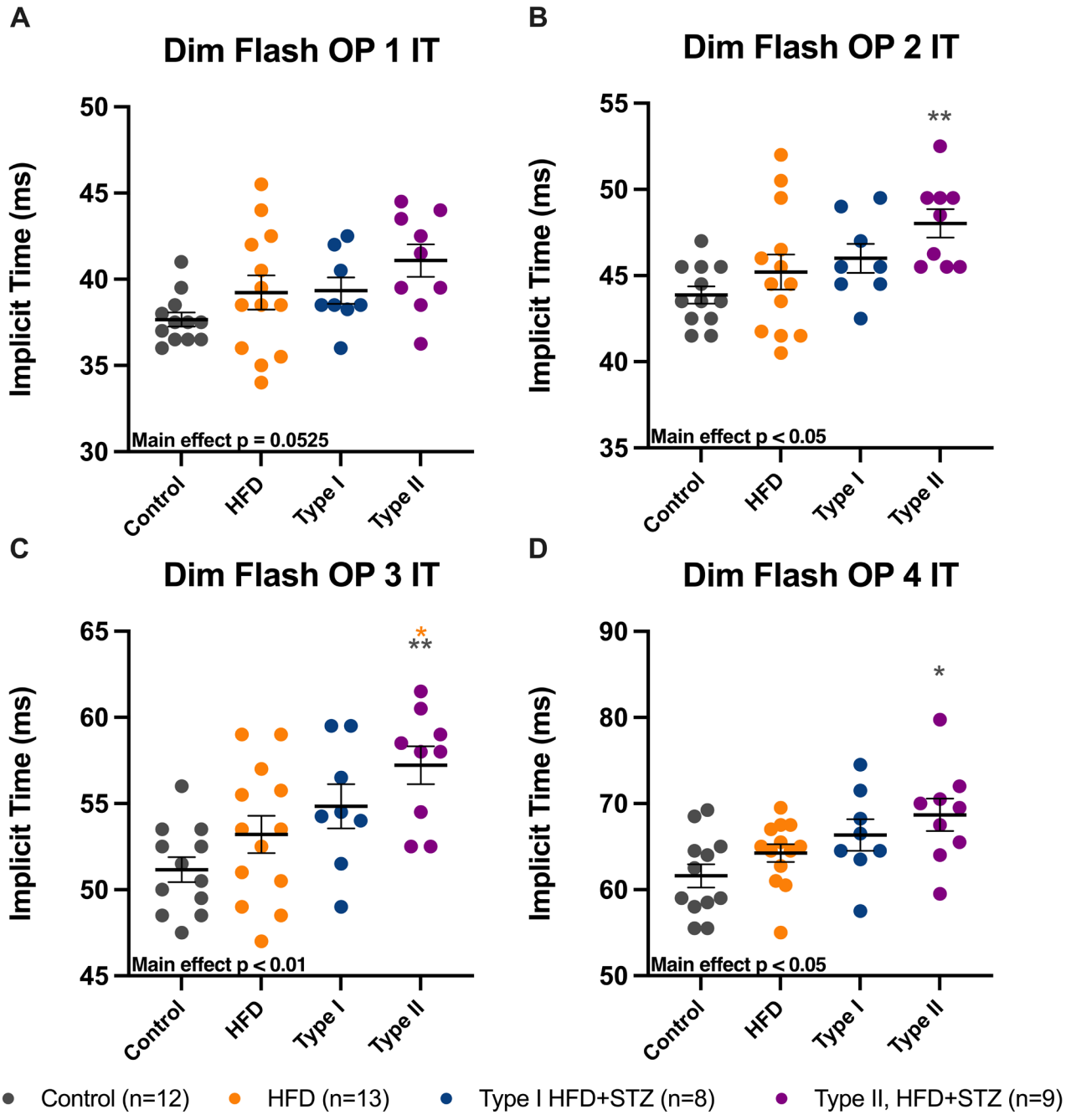

Figure 6. Type II rats showed delayed OP implicit times in OP2 through OP4 in response to dim stimuli. Oscillatory potentials taken at −1.9 log cd s/m^2 showing implicit times for OP1 (**A**), OP2 (**B**), OP3 (**C**), and OP4 (**D**) at 8 weeks post-hyperglycemia. The colored asterisks correspond to a significant difference with the group that shares the color of the asterisks. Black asterisks correspond to a significant difference with every other group. * p<0.05, ** p<0.01. Results expressed as mean ± SEM.

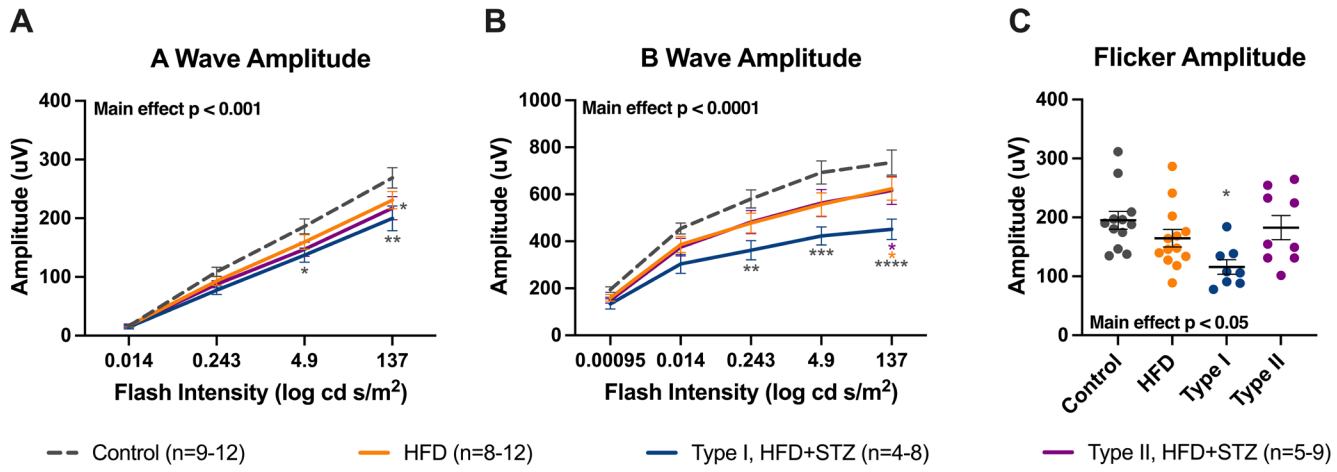

Figure 7. Type I rats showed reduced dark-adapted a- wave and b- wave amplitudes, and light-adapted flicker amplitudes. Quantification of dark-adapted a-wave (**A**) and b-wave (**B**) amplitudes and light-adapted flicker amplitudes (**C**) at 8 weeks post-hyperglycemia. The colored asterisks correspond to a significant difference with the group that shares the color of the asterisks. * p<0.05, ** p<0.01, *** p<0.001, **** p<0.0001. Results expressed as mean ± SEM.

is expected as animals on an HFD develop insulin resistance [37-39]. The diabetic state seen in these rats aligns with what is seen in humans who have Type II diabetes in terms of hyperglycemia and cells becoming resistant to insulin without a significant decrease in serum insulin [23,40].

In contrast, rats classified as Type I showed a significant loss in weight, severe hyperglycemia, and severe impairments in glucose tolerance. All of these features are commonly seen in models of Type I diabetes with increased dosage of injected STZ [29,41] and more closely resemble Type I diabetes in people.

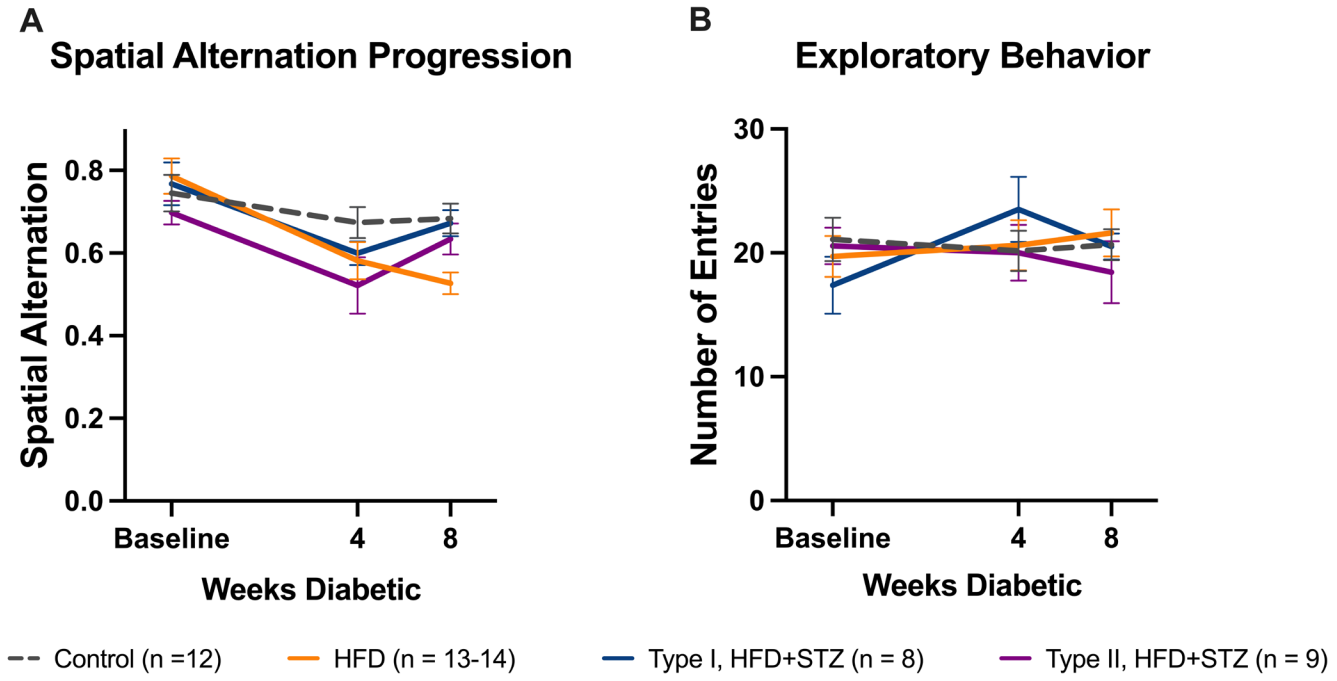

Figure 8. Differences in cognitive and exploratory behavior were not observed. Through the time points observed here, there were no significant changes observed for either spatial alternation (**A**) or exploratory behavior (**B**). Results expressed as mean ± SEM.

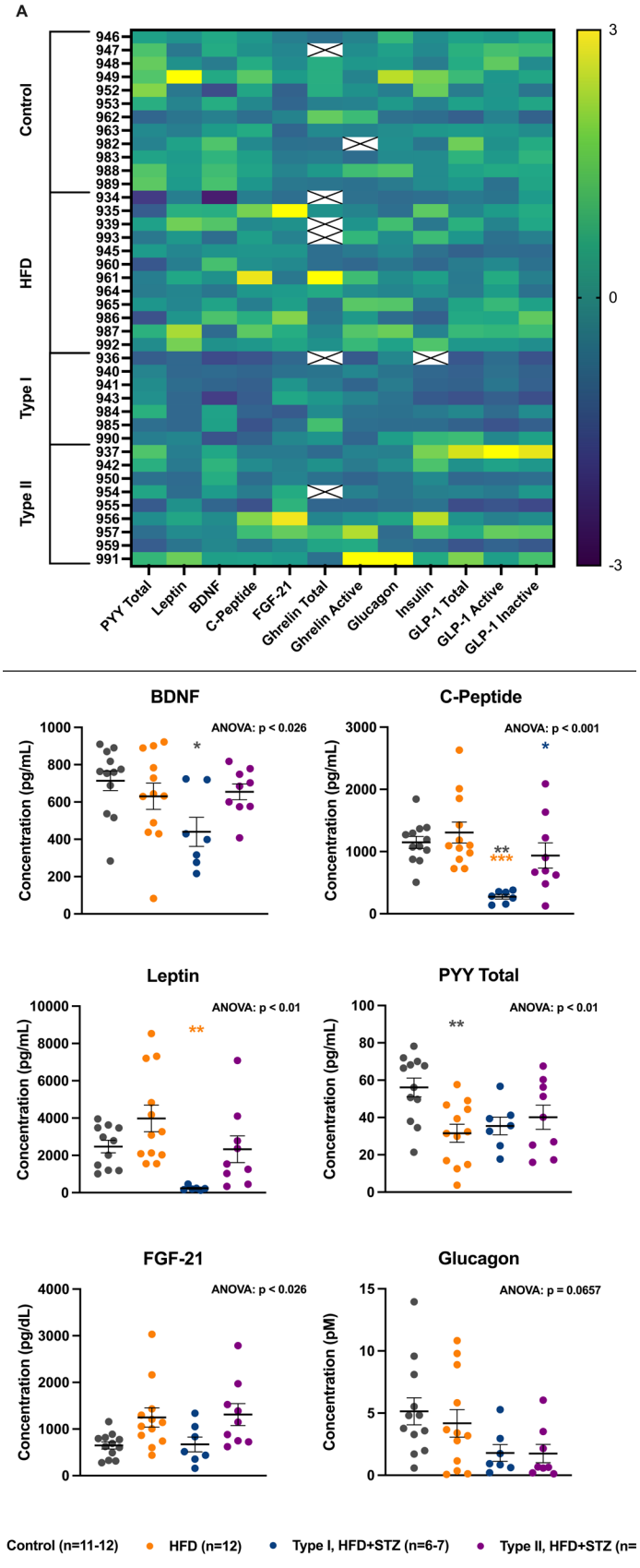

Figure 9. Type I rats showed the most prominent changes in serum biomarkers. **A**: Heatmap of z-scores for all 12 biomarkers assessed, (**B**) Serum brain-derived neurotrophic factor (BDNF) levels, (**C**) Serum C-peptide levels, (**D**) Serum leptin levels, (**E**) Serum PYY levels, (**F**) Serum FGF-21 levels, and (**G**) Serum glucagon levels evaluated by multiplex from serum collected post-euthanasia. The colored asterisks correspond to a significant difference with the group that shares the color of the asterisks. Black asterisks correspond to a significant difference with every other group. * p<0.026, ** p<0.01, *** p<0.001. Results expressed as mean ± SEM. For details on statistical analysis, including why an α level of 0.026 rather than 0.05 was used, please see the Methods section.

Type I and Type II HFD+STZ rats exhibited visual and retinal function changes typical of diabetes: Development of a Type II diabetic rat model that emulates human Type II diabetes and the retinal changes typically observed with diabetic retinopathy is necessary to better study the disease. This study is among the first to look at visual (OMR) and retinal (ERG) changes in rats being maintained on an HFD with multiple low doses of STZ. While Type II rats exhibited a more moderate diabetic state than Type I rats, they developed typical visual deficits associated with diabetic retinopathy. Type II rats

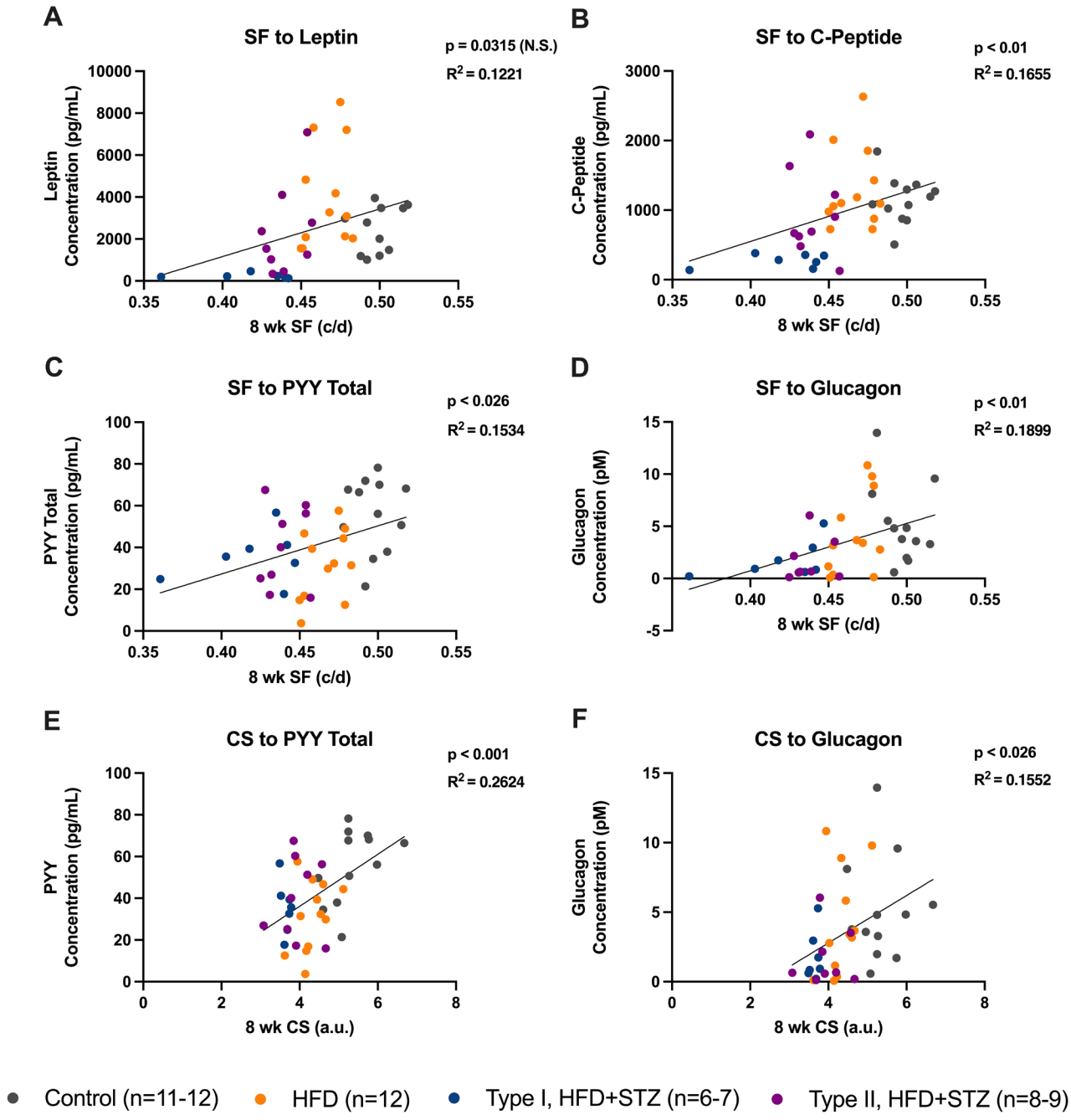

Figure 10. Serum biomarkers correlated with visual function changes, though effect sizes were small. Serum levels of metabolic biomarkers correlated with visual function data acquired at 8 weeks post-hyperglycemia. Correlation of spatial frequency with leptin (**A**), C-Peptide (**B**), PYY (**C**), and glucagon (**D**). Correlation of contrast sensitivity with PYY (E) and glucagon (**F**). Individual data points are shown for Type I HFD+STZ (blue), Type II HFD+STZ (pink), HFD only (yellow), and naïve control (gray) groups.

showed a significant decrease in visual acuity relative to naïve control (>7.45% p<0.0001) and HFD (>4.28% p<0.01) rats starting at 4 weeks post-hyperglycemia. Similarly, Type II rats showed reduced contrast sensitivity compared to naïve control (>15.64% p<0.05) rats from 4 weeks post-hyperglycemia onward. These results align with the previous literature on high-dose STZ Type I models [29,30], in which diabetic animals exhibited a significant decrease in visual acuity and contrast sensitivity. Interestingly, the HFD alone affected both spatial frequency and contrast sensitivity as well as metabolic measurements. Visual changes with an HFD have been reported in other studies such as an HFD increasing retinal vessel permeability [19,42,43]. Additionally, HFD-induced metabolic disruption is known to negatively impact retinal health through alterations to retinal fat composition, which makes the retina vulnerable to oxidative stress and inflammation [43-48].

In the case of dim oscillatory potentials, Type II rats showed a significant delay in implicit times compared to naïve controls. Delays in OP implicit times have been previously described as a marker of early diabetic retinopathy in Type I animals [25,30] as well as a sign of preclinical diabetic retinopathy in humans [25,49]. Delays in OP implicit time were not significant for Type I rats, which showed a trend for OP delays (4.35% for OP2, 7.14% for OP4), whereas significant delays have been recorded previously starting at 4 weeks in OP4 and 8 weeks in OP2 [30]. A significant delay would likely be observed with the addition of more Type I rats or later time points. There were no significant differences in implicit time for bright flash OPs, which agrees with previous findings seen in high-dose STZ Type I rats [25,30]. However, it is important to highlight that this Type I model is very different from the original high-dose Type I model (Table 1); therefore, differences in the timeline of visual and retinal impairments are not unusual. Additionally, it is possible that an HFD may actually provide a benefit to the Type I animals by helping them maintain their bodyweight.

Type I and Type II HFD+STZ rats exhibited visual changes before cognitive changes: During the time frame measured (up to 8 weeks post-STZ), no significant changes were observed in cognition or exploratory behavior as measured by spontaneous alternation and number of entries on Y-maze, respectively. The fact that visual and retinal changes occurred during this time frame suggests that retinal function changes occur before cognitive changes in diabetes. This result confirms previous findings in the Goto-Kakizaki model of Type II diabetes, in which after hyperglycemia (4 weeks), Goto-Kakizaki rats exhibited retinal function changes first, before cognitive changes, which began at 7 weeks [12]. Together, these results suggest that the retina could be useful as an early biomarker for other complications in diabetes, including cognitive changes.

The lack of cognitive changes during the time period measured could be due to two factors. First, this study followed the animals for 8 weeks post-hyperglycemia, which could be too early to detect the cognitive decline in this more moderate model of diabetes. While high-dose STZ Type I rats did show changes in Y-maze at 8 weeks post-hyperglycemia [29], the high-dose model is more severe, even compared with

Various	GK rat (Type II)	HFD+STZ rat (Type II)	HFD+STZ rat (Type I)	STZ rat (Type I)
Hyperglycemia	moderate	moderate	high	high
Source of hyperglycemia	polygenic	diet + low dose STZ	diet + low dose STZ	high dose STZ
Insulin dependent?	No	No	Occasionally	Often
ERG changes at	4 weeks	8 weeks	8 weeks	4–8 weeks
ERG amplitude	greatly increased	same as control	slightly decreased	same or slightly decreased
ERG implicit time	delayed	delayed	trend for delay	delayed
Optomotor response changes at	NA (albino)	2–4 weeks	2–4 weeks	2–4 weeks
Cognitive deficits at	6 months	—-	—-	8 weeks
Exploratory deficits at	8 weeks	—-	—-	8 weeks
Vascular function deficits	not observed by 8 months	—-	—-	2 weeks
Vascular pathology	not observed by 1 year	—-	—-	6–8 months (varies by strain)
Retinal dopamine	Increased	Not reduced (at 10 wks)	Reduced	Reduced

the HFD+STZ Type I rats in this study. In our experience, HFD+STZ Type I rats are less likely to die or to need insulin supplementation than high-dose STZ Type I rats. In general, they appear "less sick." Second, in this study, Y-maze performance was assessed at baseline and at the 4- and 8-week post-hyperglycemia time points. In our previous study in GK rats showing cognitive deficits at 7 weeks of age, the Y-maze activity was undertaken weekly instead of monthly [12]. We believe that the Y-maze performance is more sensitive when it is administered weekly, which is likely due to the rats developing a familiarity with the test. In the Goto–Kakizaki study, the control rats exhibited a small increase in spatial alternation scores from weeks 4 to 8 [12], which was not observed using monthly testing in the control rats in this study. A future direction would be to follow the animals for a longer period as well as to test Y-maze performance weekly.

HFD+STZ rats showed changes in serum levels of metabolic markers that correlated with retinal changes: We next examined several serum metabolic biomarkers in this model. Of the 12 biomarkers assessed, Type I HFD+STZ rats showed decreases in BDNF, C-Peptide, and leptin. Brain-derived neurotrophic factor is a factor that has a role in supporting neuronal function and homeostasis [50,51]. The release of BDNF is inhibited by high levels of glucose and is lower in concentration in both humans and animals with Type II diabetes [52-54]. The Type I group was the only one to show a significant decrease in BDNF levels, which could be due to the significantly higher level of hyperglycemia in this group. This decrease in BDNF has been seen in previous studies of diabetes [55,56], in both Type I [55,56] and Type II models that have drastically higher serum glucose levels than our Type II group [57,58].

C-peptide is a part of proinsulin that connects the A and B chain and is cleaved in the formation of insulin. C-peptide also binds to neuronal cells and upregulates both eNOS and Na^+/K+ ATPase activity [59,60]. As C-peptide and insulin are formed in a 1:1 ratio, the levels of C-peptide share a similar trend to what was seen in the insulin levels as measured by ELISA. The Type I group was the only one to show a significant reduction in both. This aligns with what is seen in the literature [61], as Type I diabetes is marked by a loss of β-cell function [1]. A limitation of the C-peptide results is that the serum was obtained from fed and not fasting animals with the timespan between last meal and sample collection not accounted for. There are fewer confounding variables associated with a fasting C-peptide test [62]; however, random C-peptide tests have been shown to be more advantageous in distinguishing between Type I and Type II diabetes than fasting tests [63].

Leptin is a hormone that regulates energy metabolism and energy levels and also has a role in food motivation and satiety [64]. Considering leptin is produced by adipose tissue [65,66], leptin levels have been found to be roughly proportionate to adipose content [66]. In our study, the HFD group had the highest leptin levels, with the Type I group having significantly reduced levels. This trend follows what was seen in previous literature showing higher leptin levels in HFD rats and lower leptin levels in Type I rats [67,68]. The HFD group in this study was the heaviest of the groups, whereas the Type I group had a significant drop in weight. These weight data follow previous literature as well [29,67]; however, some studies show a significant increase in weight among Type II rats [21] but not among others [20]. The combination of decreased BDNF, C-peptide, and leptin in the Type I group is interesting as these changes in metabolic markers have been previously seen in the high-dose STZ Type I model [55,56,61,68]. In Type II models, a decrease in each of these markers has previously been seen [57,58,69,70], which differs somewhat from the data presented here as the Type II rats in this study only had a significant decrease in BDNF. However, trends for differences in multiple markers were observed in the Type II rats here, and it is possible that with a larger n or a longer time course of hyperglycemia, significant differences would be observed.

While BDNF, C-Peptide, and leptin were reduced in Type I rats, PYY, which is a pancreatic polypeptide that helps regulate appetite in animals and has restorative effects on pancreatic islet function [71,72], was reduced in HFD rats. Circulating PYY levels have been shown to be decreased in GK rats [73]. Both Type I and II groups here had a nonsignificant decrease of PYY levels.

There were also two biomarkers with nonsignificant but interesting trends. Fibroblast growth factor 21 has a role in the uptake of glucose in adipocytes [74] and is elevated in people who are insulin-resistant [75]. In our study, a main effect of group was observed with the HFD and Type II groups having a nonsignificant elevation of FGF-21 levels. As for the Type I group, there was no increase. This could be due to the Type I group having more substantial damage to the liver-an off-target effect of STZ [76]—which is one of the primary locations of FGF-21 production [77]. While the Type I group experienced insulin resistance, there might have been no increase due to the elevated damage to the liver. Additionally, glucagon levels in Type I and II groups had a nonsignificant reduction. This could be due to the Type II group having less damage to the β-cells allowing the regulation of glucagon production by the α-cells [78]. Interestingly, the Type I diabetic group did not have hyperglucagonemia,

which goes against what has been seen previously [78]. This could be due to researchers in previous studies giving a higher dosage and thus causing more damage to the β-cells, impairing their regulatory relationship.

In addition to serum metabolic biomarkers showing changes in HFD+STZ animals, these changes correlated with visual and retinal changes. Specifically, serum levels of C-Peptide, PYY, and glucagon correlated with spatial frequency and serum levels of glucagon and PYY correlated with contrast sensitivity. While the effect sizes of the correlations are small, the fact that serum levels of these markers of interest correlate with the visual changes that characterize early diabetic retinopathy suggests that serum levels of C-Peptide, glucagon, and PYY could be used as biomarkers for diabetic retinopathy, potentially to identify an earlier window for treatment. However, it is important to qualify our findings in an animal model by noting that previous research in humans has shown a complicated relationship between some of these markers and diabetic retinopathy [79-81]. For instance, some human studies have shown that C-peptide has a negative relationship with vessel density [79], whereas other studies have found that residual C-peptide levels are beneficial against DR [80] and that average 30-min postprandial C-peptide levels are negatively correlated with DR progression [81]. More research is needed to assess the utilization of C-Peptide, glucagon, and PYY as biomarkers for various aspects of diabetic retinopathy.

Use of the HFD+STZ rat as a model of Type II diabetes: The high-dose STZ (100 mg/kg) model is the gold standard in modeling Type I diabetes, with its use reported in over 9,000 publications since 1963 [9,82]. The development of an inexpensive and directly analogous Type II diabetic rat model is imperative to address the growing impact of Type II diabetes throughout the world. Other commonly used Type II rodent models were considered for this study, in addition to HFD+STZ rats, but we opted not to use models that hinge on a single mutation (e.g., a leptin mutation), as they may not be as generalizable to people with diabetes. We also opted not to use the GK or Zucker diabetic fatty rats, as these animals were generated via continuous inbreeding, which we are concerned caused supernormal ERGs, increased retinal dopamine levels, and a lack of retinal vascular pathology in GK rats [12,83]. Additionally, the Zucker diabetic fatty rats exhibit alterations in nerve function that do not appear to be related to diabetes [84].

While no Type II diabetes model is as well characterized as the high-dose STZ model of Type I diabetes, the HFD+STZ rat makes an attractive model for diabetes research for the following reasons: 1) it has been widely used; 2) it relies on diet rather than a single mutation, which may be more similar to Type II diabetes in patients; 3) it models the Type II diabetic phenotype metabolically, exhibiting a moderate diabetic state with worsened glucose and insulin tolerance and higher blood glucose levels without the weight loss and insulin dependency observed in a Type I model; 4) HFD and low-dose STZ can be used in an outbred model such as Long Evans rats, allowing OMR testing, which is not possible in the albino GK strain [85,86]; and 5) the HFD+STZ rat shows retinal deficits and pathology typical of diabetes, including contrast sensitivity deficits, spatial frequency deficits, and oscillatory potential delays without the supernormal ERG amplitudes of the GK rat [12,83,87,88]. In Table 1, we provide a detailed comparison of HFD+STZ Type II rats, HFD+STZ Type I rats, GK rats, and high-dose STZ Type I rats. While we have not yet completed a long-term study showing retinal vascular pathology in the HFD+STZ rat, others have shown acellular capillaries in the retina at 9 months [87]. Following HFD+STZ Type II rats to a further time point will permit the assessment of vascular pathology and Y-maze performance.

In the high-dose STZ Type I diabetic model, visual and retinal changes have been reported that are similar to what we observed here in our Type II rats. Spatial frequency and contrast sensitivity deficits have been observed beginning at 3–4 weeks post-STZ in Type I rats [29,30] which aligns with the deficits seen in our model appearing at 2 and 3 weeks, respectively. Delays in OP implicit time are present at 3–4 weeks post-STZ [29,30,89] in the Type I model in dim conditions, while our Type II rats had significant delays at 8 weeks. This could be due to our model of Type II diabetes being a moderate diabetic state presenting with delays in OP implicit times later. The Type II animals in our study had an upper bound for blood glucose level of 250 mg/dL, whereas the Type I animals in these studies had blood glucose values above 250 mg/dL [29,30,89].

In terms of retinal vasculature, evidence of vascular function deficits at 2 weeks [90] and vascular pathology (acellular capillaries) at 6–8 months is present in the high-dose STZ Type I model [91]. Retinal vascular changes are brought on by hyperglycemia [92], and high- dose STZ rats typically exhibit higher levels of blood glucose than the rats in our study. However, acellular capillaries have also been observed in the retina of Type II rodent models, such as the db/db mouse at 11 months [93] and the Zucker diabetic fatty rat at 8 months [94]. Future studies should follow Type II HFD+STZ rats up to 8–12 months to investigate vascular pathology. Despite the Type I model being a strong model, it produces hyperglycemia through β-cell death and a subsequent drop in insulin rather than hyperglycemia being caused

by insulin resistance [9]. Although vascular pathology was not assessed in this study, following the Type II rats to a later time point and including methods such as OCT, histology, and functional hyperemia would allow us to evaluate when changes in vascular pathology occur. It is possible that morphological vascular changes will take longer to occur in this model, given the more moderate levels of hyperglycemia.

Similar studies using an HFD with multiple low doses of STZ have been reported; however, several of these studies used a higher blood glucose range for inclusion as Type II diabetic rats [70,95]. Our inclusion criteria allowed a significant increase in blood glucose levels while sustaining a larger portion of pancreatic β-cells, which is more analogous to persons with Type II diabetes [21,96]. In comparison, the Type I rats in our study, which exceeded an average blood glucose level of 250 mg/dL, had a significant and drastic reduction in their serum insulin levels, indicating more damage to the pancreas [9].

Limitations: As there are a wide range of glycemic responses to STZ [97], it is difficult to ensure that all rats fall into the Type II criteria that we used. In this study, there was a 94.4% diabetic induction rate overall, with only one rat not reaching hyperglycemia and being removed from the study. However, of the remaining rats, roughly 52.9% resulted in Type II rats. Reduction in the dosage of STZ may result in an increased number of Type II rats, but an increase in the number of injections might be needed to avoid a decline in the diabetic induction rate [95].

Streptozotocin has several off-target effects that should be considered when choosing its use in a diabetic study [76,98]. With STZ being transported by glucose transporter 2 (GLUT2) receptors [99,100], the kidneys and liver can be damaged due to the presence of these receptors and the subsequent uptake of STZ [101,102]. However, using low dose injections, as in this study, lowers the risk of off-target toxicity [76].

The low dose of STZ used in this model may also ablate a small number of islet cells in the pancreas, potentially being responsible for the lack of elevated insulin levels in the Type II HFD+STZ rats. Elevated C-Peptide levels would also be expected in Type II rodent models but were not observed in the Type II HFD+STZ rats. Future studies could address this limitation by assessing pancreatic β-cells for a Type I or Type II phenotype. This future direction could elucidate the lack of elevated insulin and C-peptide levels in the Type II HFD+STZ rats as well as the lack of elevated FGF-21 in the Type I HFD+STZ rats.

Additionally, this study only assessed male rats. This is due to the model using intravenous injection via the penile vein as the route of administration for STZ, which limits the use of the model to male animals. Experiments that characterize the HFD+STZ model and even the gold standard high-dose STZ Type I model in female rats via alternate routes of intravenous injection such as tail vein injection are critically needed in the field of diabetes research.

Conclusions: A high-fat diet together with multiple low-dose injections of STZ leads to two distinct phenotypes, with Type II rats exhibiting a moderate diabetic state characterized by moderate hyperglycemia and moderate impairment in glucose and insulin tolerance with no significant weight loss or drop in insulin levels. Despite this moderate diabetic state, Type II rats exhibited significant retinal deficits with a drop in spatial frequency, contrast sensitivity, and delayed implicit times in dim oscillatory potentials. The appearance of early visual and retinal function deficits observed here in Type I and Type II rats agrees with earlier studies showing early retinal neuronal changes before retinal vascular changes in animals and humans with diabetes. Additionally, we identified serum biomarkers that showed mild correlation with visual function changes, which could lead to their use in earlier detection and treatment of diabetic retinopathy.

ACKNOWLEDGMENTS

Conceptualization, R.S.A. and M.T.P.; methodology, S.P., A.F., J.S., L.C., A.D., K.L.B., M.C., C.T.K., C.W., and R.S.A.; formal analysis, S.P., A.F., J.S., L.C., A.D., K.L.B., M.C., L.H., C.T.K., A.G., C.W., and R.S.A.; resources, R.S.A., J.H.B., and M.T.P.; data curation, S.P., R.S.A., and M.T.P.; writing original draft preparation, S.P., A.G., J.S., A.D., L.H., and R.S.A; writing—review and editing, all co-authors; supervision, R.S.A, M.T.P, A.F., and J.H.B; project administration, R.S.A, M.T.P, A.F., and J.H.B; funding acquisition, R.S.A. and M.T.P. All authors have read and agreed to the published version of the manuscript. Funding: This research was supported by the Department of Veterans Affairs Rehab R&D Service Career Development Awards (CDA-2; RX002928) to RSA, Merit Award (RX002615) and Research Career Scientist Award (RX003134) to MTP, Career Development Award (CDA-2, RX002342) to AJF, Career Development Award (CDA-2, BX005304) to KLB, Merit Award (RX002806) to JHB; NIH NEI R01EY028859 (JHB-MTP), Core Grant P30EY006360; Research to Prevent Blindness Award to Department of Ophthalmology, Emory University; the Foundation Fighting Blindness; and the Abraham J. and Phyllis Katz Foundation. Institutional Review Board Statement: The animal study protocol was approved by the

Institutional Animal Care and Use Committee of Joseph M Cleland Atlanta VA Medical Center (protocol code: V006–22, date of approval: 05/11/2022). Informed Consent Statement: Not applicable. Data Availability Statement: The raw data supporting the conclusions of this article will be made available by the authors, without undue reservation. Acknowledgments: This study was supported in part by the Emory Multiplexed Immunoassay Core(EMIC), which is subsidized by the Emory University School of Medicine and is one of the Emory Integrated Core Facilities. Additional support was provided by the National Center for Georgia Clinical & Translational Science Alliance of the National Institutes of Health under Award Number UL1TR002378. The content is solely the responsibility of the authors and does not necessarily reflect the official views of the National Institutes of Health. Conflicts of Interest: The authors declare no conflict of interest. The funders had no role in the design of the study; in the collection, analyses, or interpretation of data; in the writing of the manuscript; or in the decision to publish the results. Prior Presentation: Presentation of part of this research was done at the 2023 ARVO meeting. Corresponding Author: Rachael Allen, restewa@emory.edu.

REFERENCES

1. . Diagnosis and Classification of Diabetes Mellitus. Diabetes Care 2010; 33:Supplement_1S62-9. [PMID: 20042775].
2. Gregory GA, Robinson TIG, Linklater SE, Wang F, Colagiuri S, de Beaufort C, Donaghue KC, Magliano DJ, Maniam J, Orchard TJ, Rai P, Ogle GD. International Diabetes Federation Diabetes Atlas Type 1 Diabetes in Adults Special Interest Group. Global incidence, prevalence, and mortality of type 1 diabetes in 2021 with projection to 2040: a modelling study. Lancet Diabetes Endocrinol 2022; 10:741-60. [PMID: 36113507].
3. Reaven GM. Role of insulin resistance in human disease (syndrome X): an expanded definition. Annu Rev Med 1993; 44:121-31. [PMID: 8476236].
4. Joussen AM, Poulaki V, Mitsiades N, Kirchhof B, Koizumi K, Döhmen S, Adamis AP. Nonsteroidal anti-inflammatory drugs prevent early diabetic retinopathy via TNF-alpha suppression. FASEB J 2002; 16:438-40. [PMID: 11821258].
5. Nathan DM, Singer DE, Godine JE, Harrington CH, Perlmuter LC. Retinopathy in older type II diabetics. Association with glucose control. Diabetes 1986; 35:797-801. [PMID: 3721064].
6. Group TDCaCTR. The Effect of Intensive Treatment of Diabetes on the Development and Progression of Long-Term Complications in Insulin-Dependent Diabetes Mellitus. https://doiorg/101056/NEJM199309303291401. 1993;329(14):977–86.
7. Yau JWY, Rogers SL, Kawasaki R, Lamoureux EL, Kowalski JW, Bek T, Chen SJ, Dekker JM, Fletcher A, Grauslund J, Haffner S, Hamman RF, Ikram MK, Kayama T, Klein BE, Klein R, Krishnaiah S, Mayurasakorn K, O'Hare JP, Orchard TJ, Porta M, Rema M, Roy MS, Sharma T, Shaw J, Taylor H, Tielsch JM, Varma R, Wang JJ, Wang N, West S, Xu L, Yasuda M, Zhang X, Mitchell P, Wong TY. Meta-Analysis for Eye Disease (META-EYE) Study Group. Global prevalence and major risk factors of diabetic retinopathy. Diabetes Care 2012; 35:556-64. [PMID: 22301125].
8. Furman BL. Streptozotocin-Induced Diabetic Models in Mice and Rats. Curr Protoc 2021; 1:e78[PMID: 33905609].
9. Junod A, Lambert AE, Orci L, Pictet R, Gonet AE, Renold AE. Studies of the diabetogenic action of streptozotocin. Proc Soc Exp Biol Med 1967; 126:201-5. [PMID: 4864021].
10. Murata M, Takahashi A, Saito I, Kawanishi S. Site-specific DNA methylation and apoptosis: induction by diabetogenic streptozotocin. Biochem Pharmacol 1999; 57:881-7. [PMID: 10086321].
11. Nahdi AMTA, John A, Raza H. Elucidation of Molecular Mechanisms of Streptozotocin-Induced Oxidative Stress, Apoptosis, and Mitochondrial Dysfunction in Rin-5F Pancreatic β-Cells. Oxid Med Cell Longev 2017; 2017:7054272[PMID: 28845214].
12. Allen RS, Feola A, Motz CT, Ottensmeyer AL, Chesler KC, Dunn R, Thulé PM, Pardue MT. Retinal Deficits Precede Cognitive and Motor Deficits in a Rat Model of Type II Diabetes. Invest Ophthalmol Vis Sci 2019; 60:123-33. [PMID: 30640976].
13. Sone H, Kawakami Y, Okuda Y, Sekine Y, Honmura S, Matsuo K, Segawa T, Suzuki H, Yamashita K. Ocular vascular endothelial growth factor levels in diabetic rats are elevated before observable retinal proliferative changes. Diabetologia 1997; 40:726-30. [PMID: 9222654].
14. Han Z, Guo J, Conley SM, Naash MI. Retinal angiogenesis in the Ins2(Akita) mouse model of diabetic retinopathy. Invest Ophthalmol Vis Sci 2013; 54:574-84. [PMID: 23221078].
15. Barber AJ, Antonetti DA, Kern TS, Reiter CEN, Soans RS, Krady JK, Levison SW, Gardner TW, Bronson SK. The Ins2Akita mouse as a model of early retinal complications in diabetes. Invest Ophthalmol Vis Sci 2005; 46:2210-8. [PMID: 15914643].
16. Lee VK, Hosking BM, Holeniewska J, Kubala EC, Lundh von Leithner P, Gardner PJ, Foxton RH, Shima DT. BTBR ob/ob mouse model of type 2 diabetes exhibits early loss of retinal function and retinal inflammation followed by late vascular changes. Diabetologia 2018; 61:2422-32. [PMID: 30094465].
17. Bogdanov P, Corraliza L, Villena J, Carvalho AR, Garcia-Arumí J, Ramos D. The db/db Mouse: A Useful Model for the Study of Diabetic Retinal Neurodegeneration. PLoS One 2014; 9:e97302.
18. Chang RC-A, Shi L, Huang CC-Y, Kim AJ, Ko ML, Zhou B, Ko GYP. High-Fat Diet-Induced Retinal Dysfunction. Invest Ophthalmol Vis Sci 2015; 56:2367-80. [PMID: 25788653].

19. Asare-Bediako B, Noothi SK, Li Calzi S, Athmanathan B, Vieira CP, Adu-Agyeiwaah Y, Dupont M, Jones BA, Wang XX, Chakraborty D, Levi M, Nagareddy PR, Grant MB. Characterizing the Retinal Phenotype in the High-Fat Diet and Western Diet Mouse Models of Prediabetes. Cells 2020; 9:464-[PMID: 32085589].

20. Reed MJ, Meszaros K, Entes LJ, Claypool MD, Pinkett JG, Gadbois TM, Reaven GM. A new rat model of type 2 diabetes: the fat-fed, streptozotocin-treated rat. Metabolism 2000; 49:1390-4. [PMID: 11092499].

21. Srinivasan K, Viswanad B, Asrat L, Kaul CL, Ramarao P. Combination of high-fat diet-fed and low-dose streptozotocin-treated rat: a model for type 2 diabetes and pharmacological screening. Pharmacol Res 2005; 52:313-20. [PMID: 15979893].

22. Huo Y, Mijiti A, Cai R, Gao Z, Aini M, Mijiti A, Wang Z, Qie R. Scutellarin alleviates type 2 diabetes (HFD/low dose STZ)-induced cardiac injury through modulation of oxidative stress, inflammation, apoptosis and fibrosis in mice. Hum Exp Toxicol 2021; 40:supplS460-74. [PMID: 34610774].

23. DeFronzo RA, Bonadonna RC, Ferrannini E. Pathogenesis of NIDDM. A balanced overview. Diabetes Care 1992; 15:318-68. [PMID: 1532777].

24. Wu L, Parhofer KG. Diabetic dyslipidemia. Metabolism 2014; 63:1469-79. [PMID: 25242435].

25. Pardue MT, Barnes CS, Kim MK, Aung MH, Amarnath R, Olson DE, Thulé PM. Rodent Hyperglycemia-Induced Inner Retinal Deficits are Mirrored in Human Diabetes. Transl Vis Sci Technol 2014; 3:6-[PMID: 24959388].

26. Pitsavos C, Tampourlou M, Panagiotakos DB, Skoumas Y, Chrysohoou C, Nomikos T, Stefanadis C. Association Between Low-Grade Systemic Inflammation and Type 2 Diabetes Mellitus Among Men and Women from the ATTICA Study. Rev Diabet Stud 2007; 4:98-104. [PMID: 17823694].

27. Kowluru RA. Retinopathy in a diet-induced type 2 diabetic rat model and role of epigenetic modifications. Diabetes 2020; 69:689-98. [PMID: 31949005].

28. Atawia RT, Bunch KL, Fouda AY, Lemtalsi T, Eldahshan W, Xu Z, Saul A, Elmasry K, Al-Shabrawey M, Caldwell RB, Caldwell RW. Role of Arginase 2 in Murine Retinopathy Associated with Western Diet-Induced Obesity. J Clin Med 2020; 9:317-[PMID: 31979105].

29. Allen RS, Hanif AM, Gogniat MA, Prall BC, Haider R, Aung MH, Prunty MC, Mees LM, Coulter MM, Motz CT, Boatright JH, Pardue MT. TrkB signalling pathway mediates the protective effects of exercise in the diabetic rat retina. Eur J Neurosci 2018; 47:1254-65. [PMID: 29537701].

30. Aung MH, Kim MK, Olson DE, Thule PM, Pardue MT. Early visual deficits in streptozotocin-induced diabetic long evans rats. Invest Ophthalmol Vis Sci 2013; 54:1370-7. [PMID: 23372054].

31. Prusky GT, Alam NM, Douglas RM. Enhancement of vision by monocular deprivation in adult mice. J Neurosci 2006; 26:11554-61. [PMID: 17093076].

32. Aung MH, Park HN, Han MK, Obertone TS, Abey J, Aseem F, Thule PM, Iuvone PM, Pardue MT. Dopamine deficiency contributes to early visual dysfunction in a rodent model of type 1 diabetes. J Neurosci 2014; 34:726-36. [PMID: 24431431].

33. Allen RS, Olsen TW, Sayeed I, Cale HA, Morrison KC, Oumarbaeva Y, Lucaciu I, Boatright JH, Pardue MT, Stein DG. Progesterone treatment in two rat models of ocular ischemia. Invest Ophthalmol Vis Sci 2015; 56:2880-91. [PMID: 26024074].

34. Turner PV, Albassam MA. Susceptibility of rats to corneal lesions after injectable anesthesia. Comp Med 2005; 55:175-82. [PMID: 15884781].

35. Maurice T, Lockhart BP, Privat A. Amnesia induced in mice by centrally administered β-amyloid peptides involves cholinergic dysfunction. Brain Res 1996; 706:181-93. [PMID: 8822355].

36. Storey JD. The positive false discovery rate: a Bayesian interpretation and the q-value. Ann Stat 2003; •••:31-.

37. Zhao S, Chu Y, Zhang C, Lin Y, Xu K, Yang P, Fan J, Liu E. Diet-induced central obesity and insulin resistance in rabbits. J Anim Physiol Anim Nutr (Berl) 2008; 92:105-11. [PMID: 18184386].

38. Flanagan AM, Brown JL, Santiago CA, Aad PY, Spicer LJ, Spicer MT. High-fat diets promote insulin resistance through cytokine gene expression in growing female rats. J Nutr Biochem 2008; 19:505-13. [PMID: 17904344].

39. Tanaka S, Hayashi T, Toyoda T, Hamada T, Shimizu Y, Hirata M, Ebihara K, Masuzaki H, Hosoda K, Fushiki T, Nakao K. High-fat diet impairs the effects of a single bout of endurance exercise on glucose transport and insulin sensitivity in rat skeletal muscle. Metabolism 2007; 56:1719-28. [PMID: 17998027].

40. Stumvoll M, Goldstein BJ, van Haeften TW. Type 2 diabetes: principles of pathogenesis and therapy. Lancet 2005; 365:1333-46. [PMID: 15823385].

41. Kaikini AA, Dhodi D, Muke S, Peshattiwar V, Bagle S, Korde A, Sarnaik J, Kadwad V, Sachdev S, Sathaye S. Standardization of type 1 and type 2 diabetic nephropathy models in rats: Assessment and characterization of metabolic features and renal injury. J Pharm Bioallied Sci 2020; 12:295-307. [PMID: 33100790].

42. Rajagopal R, Bligard GW, Zhang S, Yin L, Lukasiewicz P, Semenkovich CF. Functional Deficits Precede Structural Lesions in Mice With High-Fat Diet-Induced Diabetic Retinopathy. Diabetes 2016; 65:1072-84. [PMID: 26740595].

43. Clarkson-Townsend DA, Douglass AJ, Singh A, Allen RS, Uwaifo IN, Pardue MT. Impacts of high fat diet on ocular outcomes in rodent models of visual disease. Exp Eye Res 2021; 204:108440[PMID: 33444582].

44. Albouery M, Buteau B, Grégoire S, Martine L, Gambert S, Bron AM, Acar N, Chassaing B, Bringer MA. Impact of a high-fat diet on the fatty acid composition of the retina. Exp Eye Res 2020; 196:108059[PMID: 32387380].

45. Clarkson-Townsend DA, Bales KL, Marsit CJ, Pardue MT. Light Environment Influences Developmental Programming of the Metabolic and Visual Systems in Mice. Invest Ophthalmol Vis Sci 2021; 62:22-[PMID: 33861321].

46. Mohamed IN, Hafez SS, Fairaq A, Ergul A, Imig JD, El-Remessy AB. Thioredoxin-interacting protein is required for endothelial NLRP3 inflammasome activation and cell death in a rat model of high-fat diet. Diabetologia 2014; 57:413-23. [PMID: 24201577].

47. Kim AJ, Chang JY-A, Shi L, Chang RC-A, Ko ML, Ko GY-P. The Effects of Metformin on Obesity-Induced Dysfunctional Retinas. Invest Ophthalmol Vis Sci 2017; 58:106-18. [PMID: 28114566].

48. Marçal AC, Leonelli M, Fiamoncini J, Deschamps FC, Rodrigues MAM, Curi R, Carpinelli AR, Britto LR, Carvalho CR. Diet-induced obesity impairs AKT signalling in the retina and causes retinal degeneration. Cell Biochem Funct 2013; 31:65-74. [PMID: 22915345].

49. Motz CT, Chesler KC, Allen RS, Bales KL, Mees LM, Feola AJ, Maa AY, Olson DE, Thule PM, Iuvone PM, Hendrick AM, Pardue MT. Novel Detection and Restorative Levodopa Treatment for Preclinical Diabetic Retinopathy. Diabetes 2020; 69:1518-27. [PMID: 32051147].

50. Mattson MP, Maudsley S, Martin B. BDNF and 5-HT: a dynamic duo in age-related neuronal plasticity and neurodegenerative disorders. Trends Neurosci 2004; 27:589-94. [PMID: 15374669].

51. Lee J, Duan W, Mattson MP. Evidence that brain-derived neurotrophic factor is required for basal neurogenesis and mediates, in part, the enhancement of neurogenesis by dietary restriction in the hippocampus of adult mice. J Neurochem 2002; 82:1367-75. [PMID: 12354284].

52. Sedky AA. Improvement of cognitive function, glucose and lipid homeostasis and serum osteocalcin levels by liraglutide in diabetic rats. Fundam Clin Pharmacol 2021; 35:989-1003. [PMID: 33683755].

53. Parveen R, Kapur P, Kohli S, Agarwal NB. Attenuated brain derived neurotrophic factor and depression in type 2 diabetes mellitus patients: A case-control study. Clin Epidemiol Glob Health 2022; 15:101016.

54. Krabbe KS, Nielsen AR, Krogh-Madsen R, Plomgaard P, Rasmussen P, Erikstrup C, Fischer CP, Lindegaard B, Petersen AM, Taudorf S, Secher NH, Pilegaard H, Bruunsgaard H, Pedersen BK. Brain-derived neurotrophic factor (BDNF) and type 2 diabetes. Diabetologia 2007; 50:431-8. [PMID: 17151862].

55. Ola MS, Nawaz MI, El-Asrar AA, Abouammoh M, Alhomida AS. Reduced levels of brain derived neurotrophic factor (BDNF) in the serum of diabetic retinopathy patients and in the retina of diabetic rats. Cell Mol Neurobiol 2013; 33:359-67. [PMID: 23271640].

56. Kim ST, Chung YY, Hwang H-I, Shin H-K, Choi R, Jun YH. Differential Expression of BDNF and BIM in Streptozotocin-induced Diabetic Rat Retina After Fluoxetine Injection. In Vivo 2021; 35:1461-6. [PMID: 33910823].

57. Ahmad MF, Naseem N, Rahman I, Imam N, Younus H, Pandey SK, Siddiqui WA. Naringin Attenuates the Diabetic Neuropathy in STZ-Induced Type 2 Diabetic Wistar Rats. Life (Basel) 2022; 12:2111-[PMID: 36556476].

58. Huang L, Yan S, Luo L, Yang L. Irisin regulates the expression of BDNF and glycometabolism in diabetic rats. Mol Med Rep 2019; 19:1074-82. [PMID: 30569121].

59. Wallerath T, Kunt T, Forst T, Closs EI, Lehmann R, Flohr T, Gabriel M, Schäfer D, Göpfert A, Pfützner A, Beyer J, Förstermann U. Stimulation of endothelial nitric oxide synthase by proinsulin C-peptide. Nitric Oxide 2003; 9:95-102. [PMID: 14623175].

60. De La Tour DD, Raccah D, Jannot MF, Coste T, Rougerie C, Vague P. Erythrocyte Na/K ATPase activity and diabetes: relationship with C-peptide level. Diabetologia 1998; 41:1080-4. [PMID: 9754827].

61. Akbarzadeh A, Norouzian D, Mehrabi MR, Jamshidi Sh, Farhangi A, Verdi AA, Mofidian SM, Rad BL. Induction of diabetes by Streptozotocin in rats. Indian J Clin Biochem 2007; 22:60-4. [PMID: 23105684].

62. Maddaloni E, Bolli GB, Frier BM, Little RR, Leslie RD, Pozzilli P, Buzzetti R. C-peptide determination in the diagnosis of type of diabetes and its management: A clinical perspective. Diabetes Obes Metab 2022; 24:1912-26. [PMID: 35676794].

63. Berger B, Stenström G, Sundkvist G. Random C-peptide in the classification of diabetes. Scand J Clin Lab Invest 2000; 60:687-93. [PMID: 11218151].

64. Davis JF, Choi DL, Schurdak JD, Fitzgerald MF, Clegg DJ, Lipton JW, Figlewicz DP, Benoit SC. Leptin regulates energy balance and motivation through action at distinct neural circuits. Biol Psychiatry 2011; 69:668-74. [PMID: 21035790].

65. Zhang Y, Proenca R, Maffei M, Barone M, Leopold L, Friedman JM. Positional cloning of the mouse obese gene and its human homologue. Nature 1994; 372:425-32. [PMID: 7984236].

66. Frederich RC, Hamann A, Anderson S, Löllmann B, Lowell BB, Flier JS. Leptin levels reflect body lipid content in mice: evidence for diet-induced resistance to leptin action. Nat Med 1995; 1:1311-4. [PMID: 7489415].

67. Handjieva-Darlenska T, Boyadjieva N. The effect of high-fat diet on plasma ghrelin and leptin levels in rats. J Physiol Biochem 2009; 65:157-64. [PMID: 19886394].

68. Havel PJ, Uriu-Hare JY, Liu T, Stanhope KL, Stern JS, Keen CL, Ahrén B. Marked and rapid decreases of circulating leptin in streptozotocin diabetic rats: reversal by insulin. Am J Physiol 1998; 274:R1482-91. [PMID: 9612417].

69. Yi X, Cao S, Chang B, Zhao D, Gao H, Wan Y, Shi J, Wei W, Guan Y. Effects of acute exercise and chronic exercise on the liver leptin-AMPK-ACC signaling pathway in rats with

type 2 diabetes. J Diabetes Res 2013; 2013:946432[PMID: 24455748].

70. Akinlade OM, Owoyele BV, Soladoye AO. Streptozotocin-induced type 1 and 2 diabetes in rodents: a model for studying diabetic cardiac autonomic neuropathy. Afr Health Sci 2021; 21:719-27. [PMID: 34795728].

71. Ramracheya RD, McCulloch LJ, Clark A, Wiggins D, Johannessen H, Olsen MK, Cai X, Zhao CM, Chen D, Rorsman P. PYY-Dependent Restoration of Impaired Insulin and Glucagon Secretion in Type 2 Diabetes following Roux-En-Y Gastric Bypass Surgery. Cell Rep 2016; 15:944-50. [PMID: 27117413].

72. Chelikani PK, Haver AC, Reidelberger RD. Comparison of the inhibitory effects of PYY(3-36) and PYY(1-36) on gastric emptying in rats. Am J Physiol Regul Integr Comp Physiol 2004; 287:R1064-70. [PMID: 15242829].

73. Guida C, McCulloch LJ, Godazgar M, Stephen SD, Baker C, Basco D, Dong J, Chen D, Clark A, Ramracheya RD. Sitagliptin and Roux-en-Y gastric bypass modulate insulin secretion via regulation of intra-islet PYY. Diabetes Obes Metab 2018; 20:571-81. [PMID: 28892258].

74. Kharitonenkov A, Shiyanova TL, Koester A, Ford AM, Micanovic R, Galbreath EJ, Sandusky GE, Hammond LJ, Moyers JS, Owens RA, Gromada J, Brozinick JT, Hawkins ED, Wroblewski VJ, Li DS, Mehrbod F, Jaskunas SR, Shanafelt AB. FGF-21 as a novel metabolic regulator. J Clin Invest 2005; 115:1627-35. [PMID: 15902306].

75. Chavez AO, Molina-Carrion M, Abdul-Ghani MA, Folli F, Defronzo RA, Tripathy D. Circulating fibroblast growth factor-21 is elevated in impaired glucose tolerance and type 2 diabetes and correlates with muscle and hepatic insulin resistance. Diabetes Care 2009; 32:1542-6. [PMID: 19487637].

76. Koulmanda M, Qipo A, Chebrolu S, O'Neil J, Auchincloss H, Smith RN. The effect of low versus high dose of streptozotocin in cynomolgus monkeys (Macaca fascilularis). Am J Transplant 2003; 3:267-72. [PMID: 12614280].

77. Nishimura T, Nakatake Y, Konishi M, Itoh N. Identification of a novel FGF, FGF-21, preferentially expressed in the liver. Biochim Biophys Acta 2000; 1492:203-6. [PMID: 10858549].

78. Feng AL, Xiang Y-Y, Gui L, Kaltsidis G, Feng Q, Lu W-Y. Paracrine GABA and insulin regulate pancreatic alpha cell proliferation in a mouse model of type 1 diabetes. Diabetologia 2017; 60:1033-42. [PMID: 28280900].

79. Qi Z, Si Y, Feng F, Zhu J, Yang X, Wang W, Zhang Y, Cui Y. Analysis of retinal and choroidal characteristics in patients with early diabetic retinopathy using WSS-OCTA. Front Endocrinol (Lausanne) 2023; 14:1184717[PMID: 37293481].

80. Harsunen M, Haukka J, Harjutsalo V, Mars N, Syreeni A, Härkönen T, Käräjämäki A, Ilonen J, Knip M, Sandholm N, Miettinen PJ, Groop PH, Tuomi T. Residual insulin secretion in individuals with type 1 diabetes in Finland: longitudinal and cross-sectional analyses. Lancet Diabetes Endocrinol 2023; 11:465-73. [PMID: 37290465].

81. Pan T, Gao J, Cai X, Zhang H, Lu J, Lei T. The average 30-minute post-prandial C-peptide predicted diabetic retinopathy progress: a retro-prospective study. BMC Endocr Disord 2023; 23:63-[PMID: 36922809].

82. Rakieten N, Rakieten ML, Nadkarni MV. Studies on the diabetogenic action of streptozotocin (NSC-37917). Cancer Chemother Rep 1963; 29:91-8. .

83. Allen RS, Khayat CT, Feola AJ, Win AS, Grubman AR, Chesler KC, He L, Dixon JA, Kern TS, Iuvone PM, Thule PM, Pardue MT. Diabetic rats with high levels of endogenous dopamine do not show retinal vascular pathology. Front Neurosci 2023; 17:1125784[PMID: 37034167].

84. Hempe J, Elvert R, Schmidts HL, Kramer W, Herling AW. Appropriateness of the Zucker Diabetic Fatty rat as a model for diabetic microvascular late complications. Lab Anim 2012; 46:32-9. [PMID: 22087029].

85. Braha M, Porciatti V, Chou TH. Retinal and cortical visual acuity in a common inbred albino mouse. PLoS One 2021; 16:e0242394.

86. Precht W, Cazin L. Functional deficits in the optokinetic system of albino rats. Exp Brain Res 1979; 37:183-6. [PMID: 488214].

87. Mancini JE, Ortiz G, Croxatto JO, Gallo JE. Retinal upregulation of inflammatory and proangiogenic markers in a model of neonatal diabetic rats fed on a high-fat-diet. BMC Ophthalmol 2013; 13:14-[PMID: 23587252].

88. Ren X, Li C, Liu J, Zhang C, Fu Y, Wang N, Ma H, Lu H, Kong H, Kong L. Thioredoxin plays a key role in retinal neuropathy prior to endothelial damage in diabetic mice. Oncotarget 2017; 8:61350-64. [PMID: 28977868].

89. Chesler K, Motz C, Vo H, Douglass A, Allen RS, Feola AJ, Pardue MT. Initiation of L-DOPA Treatment After Detection of Diabetes-Induced Retinal Dysfunction Reverses Retinopathy and Provides Neuroprotection in Rats. Transl Vis Sci Technol 2021; 10:8-[PMID: 34003986].

90. Aung MH, Kim MK, Thule PM, Pardue MT. Assessing Flicker-induced Retinal Vascular Responses using Scanning Laser Ophthalmoscope. Invest Ophthalmol Vis Sci 2012; 53:5434-.

91. Kern TS, Miller CM, Tang J, Du Y, Ball SL, Berti-Matera L. Comparison of three strains of diabetic rats with respect to the rate at which retinopathy and tactile allodynia develop. Mol Vis 2010; 16:1629-39. [PMID: 20806092].

92. Klein R, Klein BE, Moss SE, Cruickshanks KJ. Relationship of hyperglycemia to the long-term incidence and progression of diabetic retinopathy. Arch Intern Med 1994; 154:2169-78. [PMID: 7944837].

93. Beli E, Yan Y, Moldovan L, Vieira CP, Gao R, Duan Y, Prasad R, Bhatwadekar A, White FA, Townsend SD, Chan L, Ryan CN, Morton D, Moldovan EG, Chu FI, Oudit GY, Derendorf H, Adorini L, Wang XX, Evans-Molina C, Mirmira RG, Boulton ME, Yoder MC, Li Q, Levi M, Busik JV, Grant MB. Restructuring of the Gut Microbiome by Intermittent Fasting

Prevents Retinopathy and Prolongs Survival in *db/db* Mice. Diabetes 2018; 67:1867-79. [PMID: 29712667].

94. Wohlfart P, Lin J, Dietrich N, Kannt A, Elvert R, Herling AW, Hammes H-P. Expression patterning reveals retinal inflammation as a minor factor in experimental retinopathy of ZDF rats. Acta Diabetol 2014; 51:553-8. [PMID: 24477469].

95. Zhang M, Lv XY, Li J, Xu ZG, Chen L. The characterization of high-fat diet and multiple low-dose streptozotocin induced type 2 diabetes rat model. Exp Diabetes Res 2008; 2008:704045[PMID: 19132099].

96. King AJ. The use of animal models in diabetes research. Br J Pharmacol 2012; 166:877-94. [PMID: 22352879].

97. Kramer J, Moeller EL, Hachey A, Mansfield KG, Wachtman LM. Differential expression of GLUT2 in pancreatic islets and kidneys of New and Old World nonhuman primates. Am J Physiol Regul Integr Comp Physiol 2009; 296:R786-93. [PMID: 19073904].

98. Foster SR, Dilworth LL, Omoruyi FO, Thompson R, Alexander-Lindo RL. Pancreatic and renal function in streptozotocin-induced type 2 diabetic rats administered combined inositol hexakisphosphate and inositol supplement. Biomed Pharmacother 2017; 96:72-7. [PMID: 28965010].

99. Schnedl WJ, Ferber S, Johnson JH, Newgard CB. STZ transport and cytotoxicity. Specific enhancement in GLUT2-expressing cells. Diabetes 1994; 43:1326-33. [PMID: 7926307].

100. Hosokawa M, Dolci W, Thorens B. Differential sensitivity of GLUT1- and GLUT2-expressing β cells to streptozotocin. Biochem Biophys Res Commun 2001; 289:1114-7. [PMID: 11741307].

101. Wood IS, Trayhurn P. Glucose transporters (GLUT and SGLT): expanded families of sugar transport proteins. Br J Nutr 2003; 89:3-9. [PMID: 12568659].

102. Thorens B, Sarkar HK, Kaback HR, Lodish HF. Cloning and functional expression in bacteria of a novel glucose transporter present in liver, intestine, kidney, and β-pancreatic islet cells. Cell 1988; 55:281-90. [PMID: 3048704].

Articles are provided courtesy of Emory University and the Zhongshan Ophthalmic Center, Sun Yat-sen University, P.R. China. The print version of this article was created on 1 July 2024. This reflects all typographical corrections and errata to the article through that date. Details of any changes may be found in the online version of the article.